

Layer Frustration, Polar Order and Chirality in Liquid Crystalline Phases of Silyl-Terminated Achiral Bent-Core Molecules

Christina Keith,^[a] Ramaiahgari Amaranatha Reddy,^[a, d] Marko Prehm,^[a] Ute Baumeister,^[b] Horst Kresse,^[b] Jessie Lorenzo Chao,^[b] Harald Hahn,^[c] Heinrich Lang,^[c] and Carsten Tschierske*^[a]

Abstract: A novel class of bent-core molecules with oligo(siloxane) or carbosilane units at both ends was synthesized and the self-organization of these molecules was investigated by polarizing microscopy, DSC, X-ray scattering, dielectric and electrooptical methods. Depending on the size of the silicon-containing segments, smectic and columnar liquid crystalline phases are formed. Most smectic phases are low birefringent and composed of macroscopic domains of opposite handedness (dark conglomerate phases). The switching process in these smectic

phases is surface stabilized ferroelectric and, depending on the conditions, two distinct slow relaxation processes to nonpolar structures were observed. It is proposed that the smectic phases are built up by chiral and polar SmC_sP_F layer stacks which are separated by anticlinal interfaces. If the size of these layer stacks is sufficiently large a coupling to the substrate surfaces takes

place and ferroelectric switching is observed. It is also suggested that the sponge-like layer distortion, occurring in the low birefringent mesophases, is due to an escape from the local polar order within these SmC_sP_F layer stacks. For compounds with larger silylated units a steric frustration arises, which leads to layer modulation (columnar ribbon phases) and this is associated with a transition from ferroelectric to antiferroelectric switching. All compounds show a switching of the molecules around the long axis which reverses the layer chirality.

Keywords: ferroelectricity • liquid crystals • mesophases • self-assembly • supramolecular chemistry

Introduction

The design of programmed molecules which can organize in a predictable way with formation of complex superstructures is an attractive target of contemporary research.^[1] Crystal engineering, for example, has significantly advanced during the last decade by using rigid molecules having a well defined shape and functionality.^[2] Such molecules play an important role in coordination polymers and metal-organic frameworks,^[3] as well as for the construction of polygonal grids^[4] and cage structures.^[5] Moreover, rigid segments are important building blocks for liquid crystalline (LC) materials.^[6] In all these cases the shape of the rigid segments and their appropriate functionalization determine the morphology of the resulting self-assembled superstructure. Chevron-shaped molecules, for example, can be organized in quite different modes, such as supramolecular rhombuses, hexagons, helical superstructures,^[7–9] zigzag patterns^[10] (Figure 1) or cages.^[11] Another mode of organization is the formation of densely packed layers or ribbons with a uniform direction of the chevrons (see bottom of Figure 1). These systems exhibit LC properties if flexible alkyl chains are attached to

[a] Dr. C. Keith, Dr. R. Amaranatha Reddy, Dipl.-Chem M. Prehm, Prof. Dr. C. Tschierske
Institute of Organic Chemistry
Martin-Luther-University Halle-Wittenberg
Kurt-Mothes-Strasse 2, 06120 Halle (Germany)
Fax: (+49)345-552-7346
E-mail: carsten.tschierske@chemie.uni-halle.de

[b] Dr. U. Baumeister, Prof. Dr. H. Kresse, Dipl.-Chem J. L. Chao
Institute of Physical Chemistry
Martin-Luther-University Halle-Wittenberg, Mühlport
06108 Halle (Germany)

[c] Dr. H. Hahn, Prof. Dr. H. Lang
Faculty of Sciences, Department of Chemistry
Institute of Inorganic Chemistry
Strasse der Nationen 62, 09111 Chemnitz (Germany)

[d] Dr. R. Amaranatha Reddy
present address:
Department of Chemistry and Biochemistry
University of Colorado at Boulder, Boulder, CO 80309-0215 (USA)

Supporting information for this article is available on the WWW under <http://www.chemeurj.org/> or from the author: Additional figures and table with X-ray data.

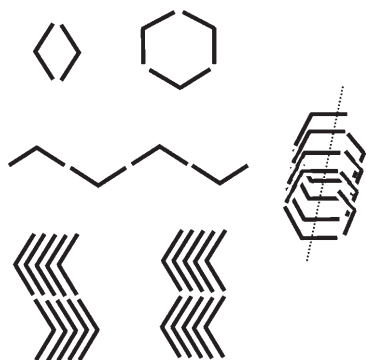


Figure 1. Examples of supramolecular structures formed by chevron-like molecules. These structures can be found in coordination polymers, discrete supramolecular aggregates, etc. The individual molecules can be organized, for example, by metal coordination, hydrogen bonding or van der Waals forces.

the ends of the rigid units. Liquid crystals (LC) have important application properties as these materials can easily change their configuration under the influence of different external stimuli. This unique combination of long range order and local mobility provides the foundation of numerous technological applications of such materials, as for example in display devices.^[6]

Within the field of LC materials chevron-shaped molecules, usually designated as bent-core LC or banana-shaped LC, are of special current interest.^[12,13] For such molecules a polar order results from the packing of the bent-core units in layers where the bent structure restricts their rotation around the long axis, leading to a directed packing with a polar direction (P) parallel to the layer planes, giving rise to polar smectic phases (SmP). Remarkably, in most cases, the molecules are additionally tilted in these polar layers and this increases the structural diversity in these self-organized systems. In adjacent layers tilt direction and polar direction can be either identical or opposite, leading to in total four different phase structures, as shown in Figure 2.^[14] Two of them are macroscopically polar, assigned as ferroelectric (SmC_sP_F and SmC_aP_F), the others are macroscopically non-polar and assigned as antiferro-

electric (SmC_aP_A and SmC_sP_A). Usually the antiferroelectric states (SmC_aP_A and SmC_sP_A) are more stable and can be switched into the corresponding ferroelectric states (SmC_sP_F and SmC_aP_F respectively) under the influence of an external electric field. Upon switching off the field the polar ferroelectric (FE) states usually relax back to the nonpolar antiferroelectric (AF) states. This switching process includes three stable states and is therefore assigned as an AF switching process. In few special materials, however, the switching can take place by a direct switching between the two polar FE states without relaxation to an AF state, which is assigned as FE switching.^[15] Hence, these bent-core LC provide a new source of polar ordered soft matter with FE and AF properties.

In addition, the tilted organization of these achiral molecules in polar layers gives rise to a C₂ symmetry of the layers, which lacks a mirror symmetry and therefore these layers are inherently chiral, providing a new source of supramolecular chirality (more specific: superstructural chirality).^[14] Layer normal, tilt direction and polarization vector describe either a right handed or a left handed system (see Figure 2c). Changing either the direction of the polarization

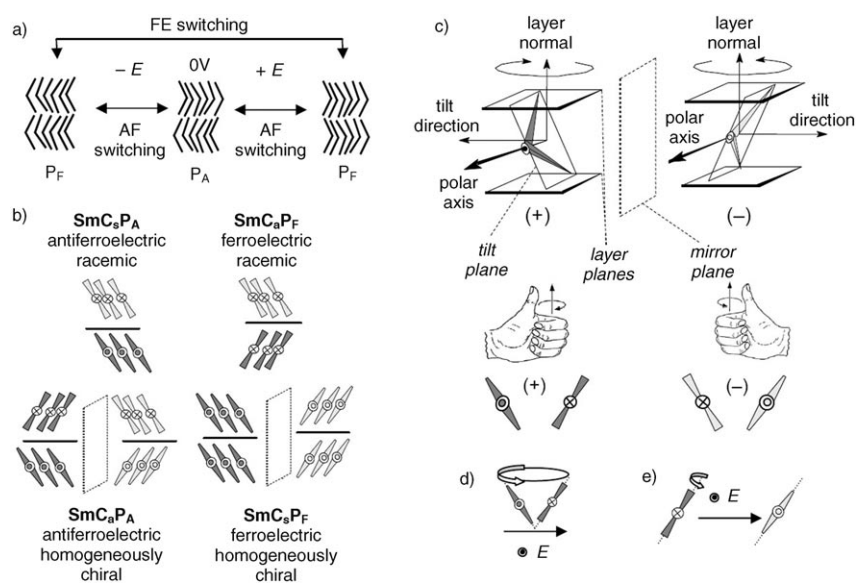


Figure 2. Organization of bent-core molecules in polar smectic phases: a) FE and AF switching of bent-core molecules (side views). b) The four classical arrangements in tilted polar smectic phases. The subscripts “s” and “a” indicate the correlation of the tilt direction in adjacent layers: s = synclinal means an identical tilt direction; a = anticlinal indicates an opposite tilt direction. Subscripts “A” and “F” indicate the correlation of the polar direction in adjacent layers. P_A is indicative for an antipolar structure (polar direction alternates); this structure is macroscopically nonpolar and usually assigned as “antiferroelectric”. P_F stands for a synpolar structure (polar direction is identical); this structure is macroscopically polar and usually assigned as “ferroelectric” (P_F). The grey-scale indicates the chirality of the layers. The SmC_aP_A and SmC_sP_F structures are homogeneously chiral (identical chirality sense in the layers), the SmC_sP_A and SmC_aP_F structures are macroscopically racemic (alternating chirality sense in the layers). Only two layers are shown to represent the structure, but in these classical models the indicated alternation of polar order or tilt direction takes place between each of the individual layers. c) Origin of the superstructural chirality within the smectic phases of bent-core molecules. Layer normal, tilt direction and the polar axis define either a right-handed coordinate system (+) shown in dark grey, whereas in the mirror image these vectors define a left-handed system (-), shown in pale grey. This code is maintained throughout the manuscript. d) Switching on a cone reverses polar direction and tilt direction and hence, retains the layer chirality. e) Switching around the long axes of the molecules reverses only the polar direction and in this way reverses layer chirality.

or the tilt direction changes the chirality sense of the layers, whereas changing both retains the chirality sense. The SmC_sP_A and SmC_aP_F phases have opposite chirality sense in adjacent layers, leading to macroscopically racemic superstructures, whereas in the SmC_aP_A and SmC_sP_F phases the layers have identical chirality sense and hence, these structures are homogeneously chiral and a mirror image exists for each of these structures (see Figure 2b). In the (+)- and (-)- SmC_sP_F phases, for example, either the tilt direction or the polar direction is opposite (see Figure S1, Supporting Information). The polar direction can be reversed by means of electric fields and for this collective process there are two distinct switching mechanisms. If the switching takes place by collective rotation on a cone, which is usually the case, tilt direction and polar direction are changed simultaneously and layer chirality is preserved (see Figure 2d).^[14] However, if the molecules reorganize by a collective rotation around the long axis, only the polar direction is reversed and this gives rise to an inversion of the layer chirality (see Figure 2e). This provides the possibility of field induced transitions from a racemic to a uniformly chiral structure and for homogeneously chiral structures the chirality sense can be reversed by means of electric fields.^[16,17] This unique combination of properties makes this new class of LC materials especially interesting for numerous applications, for example as switchable ferroelectric, NLO active and chiroptical materials.^[18]

We have recently enhanced the complexity of bent-core molecules by introduction of oligosiloxane and carbosilane units.^[19] It turned out that such silyl groups have a significant impact on the properties of the mesophases of these molecules. These units change the switching behavior from AF to FE and also the optical appearance of the mesophase is completely changed. The highly birefringent textures usually observed for smectic phases of bent-core molecules with simple alkyl chains, like **I** (Figure 3) are replaced by low birefringent or optically isotropic phases which appear dark between crossed polarizers. Moreover, these mesophases are composed of a 1:1 mixture of macroscopically chiral domains with opposite handedness.^[19] In crystalline systems this type of racemic structure, where enantiomers are organized in separate enantiomorphous crystals is termed conglomerate.^[20] Hence, this type of low-birefringent mesophases

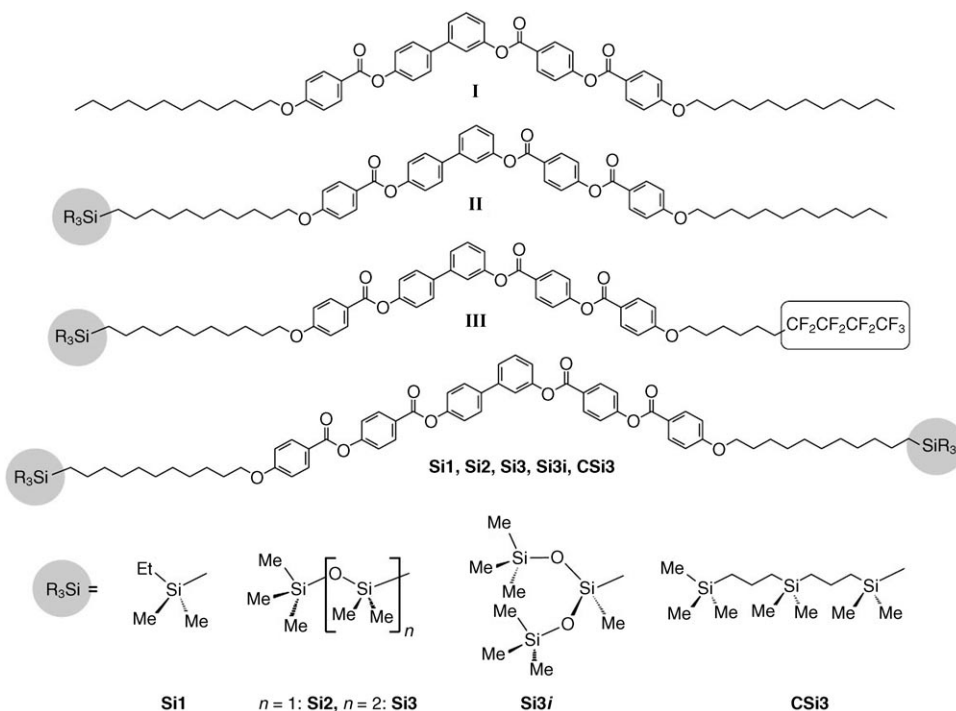


Figure 3. Comparison of the structures of distinct types of bent-core molecules: classical bent-core molecules **I**,^[24] bent-core molecules having only one silyl unit (compounds **II**),^[19a-f] bent-core molecules having silyl and perfluoroalkyl end groups (compounds **III**),^[19g] the molecules **Si1–CSi3**, having silyl groups at both ends are reported herein.^[16]

with a local chiral structure has been assigned as “dark conglomerate phase” and is indicated by the superscript “[*]”, which indicates that the mesophase has a chiral superstructure though the molecules themselves are achiral.^[21] These mesophases have been found for few distinct classes of bent-core materials,^[22,23] but in the class of silylated bent-core molecules they are dominating.^[19] Neither the origin of ferroelectricity in some of these mesophases, nor the origin of the spontaneous achiral symmetry breaking with formation of macroscopic homogeneously chiral domains, nor the driving forces for layer distortion, leading to optical isotropy of these smectic phases are fully understood at present.

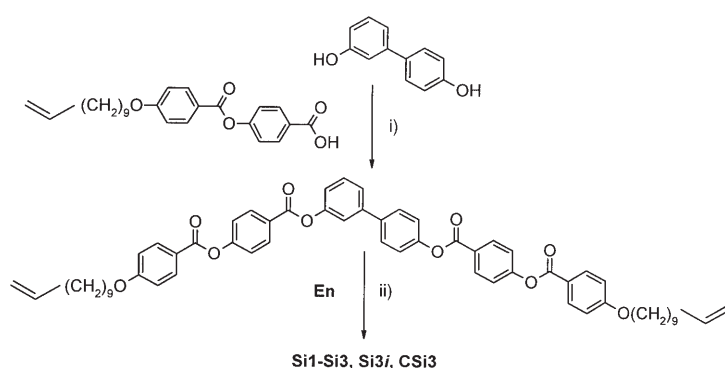
Herein we propose a model of the “dark conglomerate phases” found for the silylated bent-core molecules, based on a mesophase structure composed of chiral and polar mesoscale SmC_sP_F layer stacks. It is suggested that ferroelectricity arises due to surface coupling which occurs if these polar SmC_sP_F layer stacks exceed a certain critical size, and that layer distortion is due to the escape from the mesoscale polarity within these polar layer stacks. The investigations were done with a new class of bent-core mesogens, namely compounds **Si1–Si3**, **Si3i** and **CSi3** with structures shown in Figure 3. In contrast to the earlier reported compounds with only one silyl group^[19] these molecules have silicon containing groups at both ends, which has a significant impact upon their self-organization, due to the segregation, the layer decoupling and steric effects of the silyl groups.^[19] Some of the materials show a temperature dependent change of the

mode of molecular self organization from a sponge-like net of layers in the “dark conglomerate phases” to ribbon-like aggregates in the modulated smectic (columnar phases). This is associated with a change of the switching process from FE to AF. Moreover, in most mesophases formed by these molecules, switching takes place by rotation around the long axis which switches the chirality of the LC system. The generalization of these results improves the knowledge about the self organization principles in polar soft matter systems, providing fundamental clues for a target specific design of new bent-core mesogenic materials.

Results and Discussion

Synthesis

The synthesis of compound **En** with two terminal double bonds was achieved by esterification of 3,4'-biphenyldiol^[24] with 4-[4-(10-undecenyloxy)benzoyloxy]benzoic acid (see Schem 1).^[25,26] In the final step **En** was hydrosilylated with appropriate H-silanes according to procedures described earlier, yielding the siloxane derivatives **Si2–Si3**, **Si3i**^[16] and the carbosilanes **Si1** and **CSi3**.^[19] Isolation and purification was achieved by repeated chromatography and crystallization.



Scheme 1. Synthesis of compounds **Si1–Si3**, **Si3i** and **CSi3**: i) DCC, DMAP, CH₂Cl₂, 20 °C, 24 h;^[26] ii) EtMe₂SiH (**Si1**), Me₃Si(OMe₂Si)_nH (n = 1, 2: **Si2**, **Si3**), or (Me₃SiO)₂MeSiH (**Si3i**), or Me₃Si[(CH₂)₃Me₂Si]₂H (**CSi3**), Karstedt's catalyst, toluene, 20 °C, 24 h.^[19] DCC = dicyclohexylcarbodiimide, DMAP = dimethylaminopyridine.

Investigation of the LC behaviour—Comparison of the olefin terminated compound **En** with the silylated molecules **Si_n**

The synthesized compounds were investigated by polarizing microscopy, differential scanning calorimetry (DSC), X-ray diffraction and by detailed electrooptical investigations. In Table 1 the influence of the size of the Si-containing units upon the liquid crystalline properties is shown.

The nonsilylated and terminally unsaturated compound **En** shows the typical textural features of the so-called B1 phases (see Figure 4a,b). This is a rectangular columnar

phase (Col_r) composed of ribbons with an antipolar order of the ribbons in a 2D lattice ($a = 3.9$, $b = 4.9$ nm), which is stabilized by the efficient escape from a macroscopic polar order provided by this organization.^[27] As most B1 phases, also the columnar phase of **En** does not show any polar switching. In this Col_r phase the terminal chains are in contact with the bent aromatic cores at the interfaces between the ribbons (see Figure 4c). Silylation of the terminal double bonds gives rise to an increase of the incompatibility of the terminal chains with these cores, which destabilizes the ribbon-like organization. Therefore, this columnar phase is replaced by a layer structure (SmCP_{FE}^[*]) without these unfavorable inter-ribbon interfaces, if ethyldimethylsilyl units (compound **Si1**) or pentamethyldisiloxane-1-yl units (compound **Si2**) are attached to both ends. For compounds with larger silicon-containing groups (heptamethyltrisiloxane units in compounds **Si3** and **Si3i**^[16,28] and carbosilane units in **CSi3**), however, a steric frustration arises within the layers and the layer structure becomes frustrated again. This steric frustration leads to oblique columnar phases (Col_{ob}, Col_{ob}P_A), which replace the smectic phases.

Smectic phases of compounds **Si1** and **Si2**

Investigation of the ground-state structures: For compounds **Si1** and **Si2** X-ray investigations indicate a smectic phase without in-plane order over the whole mesomorphic temperature range. The layer distance, determined by X-ray scattering, is significantly smaller than the calculated molecular length and this is in line with a tilted organization of the molecules in these smectic phases. Only one maximum of the diffuse scattering at $d = 0.46$ nm is observed for **Si1** with ethyldimethylsilyl end groups (see Figure S2a, Supporting Information), whereas the wide angle region of **Si2** is characterized by a diffuse scattering with two maxima (see Figure S2b, Supporting Information), one at $d = 0.45$ nm corresponds to the mean distance between the alkyl and the aryl segments, and a second one corresponding to $d = 0.63$ nm, assigned to the mean distance between the nano-segregated pentamethyldisiloxane units. The model of the organization of **Si2** in the smectic phase is shown in Figure 5b. Due to the segregation of the terminal silyl groups there are two different mean distances between the hydrocarbon units (cross-sectional area = 0.21 nm²) and between the siloxane units (cross-sectional area = 0.38 nm²) which leads to a steric frustration within these layers. Tilting of the aromatic units and folding of the alkyl chains can partly compensate this difference, but nevertheless it can be assumed that the packing of the aromatic cores and alkyl chains is disturbed in comparison to conventional bent-core mesogens and in comparison to the monosilylated compounds **II** where antiparallel packing can compensate this difference (Figure 5a).^[19f,29]

Upon cooling compounds **Si1** and **Si2** between crossed polarizers, the mesophases appear as fractal nuclei which coalesce to grainy unspecific and low-birefringent textures (see Figure 6b). Upon rotating the analyzer by small angle (5–

Table 1. Mesophases, phase transition temperatures, transition enthalpies and lattice parameters of the bent-core molecules under investigation.^[a]

R ₃ Si	T/°C					d, a, b/nm, γ/°	l/nm ^[c]
	ΔH/kJ mol ⁻¹ [b]						
En	--	Cr 99 43.6	Col _r 146 Iso 18.8			a = 3.9, b = 4.9 (125 °C)	5.6
Si1	EtMe ₂ Si-	Cr 111 46.2	SmCP _{FE} ^[*] 159 Iso 27.1			4.4 (120 °C)	6.2
Si2	Me ₃ SiOMe ₂ Si-	Cr 80 14.8	SmCP _{FE} ^[*] 162 Iso 26.0			4.5 (95 °C)	6.6
Si3	Me ₃ Si(OMe ₂ Si) ₂ -	Cr 89 10.5	SmCP _{FE} 126 <0.1	SmCP _A 143 ^[d] 1.0	Col _{ob} P _A 147 ^[e] -	Col _{ob} 155 Iso 20.7	d = 4.8 (120 °C) a = 5.8, b = 5.1, γ = 114.5 (148 °C)
Si3i	(Me ₃ SiO) ₂ MeSi-	Cr 78 12.7	USmCP _A 127 1.3	Col _{ob} P _A 157 Iso ^[f] 24.0		d = 4.7 (110 °C) a = 2.5, b = 4.65, γ = 107 (130 °C) ^[g]	6.6
CSI3	Me ₃ Si[(CH ₂) ₃ Me ₂ Si] ₂ -	Cr 60 7.2	SmCP _{FE} 132 ^[h] -	SmCP _A 139 1.7	Col _{ob} P _A 150 Iso 17.0	d = 5.1 (120 °C) a = 2.8, b = 5.1, γ = 108 (144 °C)	7.8

[a] Peak temperatures, determined by DSC, first heating scan, 10 K min⁻¹; abbreviations: Col_r=nonswitchable rectangular columnar phase (B1-type phase); SmCP_{FE}=FE switching and birefringent polar smectic phase, SmCP_{FE}^[*]=FE switching dark conglomerate phase, ^[*] indicates the formation of optically active domains, though the molecules themselves are achiral, the virgin ground-state structure in both SmCP_{FE} phases is assumed to be [SmC₃P_F]_aP_A (see Figure 8c); SmCP_A=AF switching smectic phase; USmCP_A=AF switching undulated smectic phase; Col_{ob}=nonswitching oblique columnar phase; Col_{ob}P_A=AF switching oblique columnar phase. [b] Values in the lower lines in italics. [c] Determined using CPK models and assuming a V-shape with a bending angle of 120° and a most stretched conformation of the rod-like wings (alkyl chains in all-trans conformation). [d] Phase transition on cooling: 136 °C. [e] Determined by electrooptical investigations in a polyimide coated ITO cell (6 μm). [f] See ref. [16], the slightly higher transition temperatures in comparison to the reference values are due to the higher purity of the 1,1,1,2,3,3,3-heptamethyltrisiloxane used for the repeated synthesis of this compound. [g] See ref. [28]. [h] Determined by electrooptical investigations in a noncoated ITO cell (6 μm) on heating, on cooling the phase transition is seen at 127 °C; a peak at T = 127 °C (ΔH = 1.4 kJ mol⁻¹) is also seen in the DSC cooling curve, but not in the heating scan.

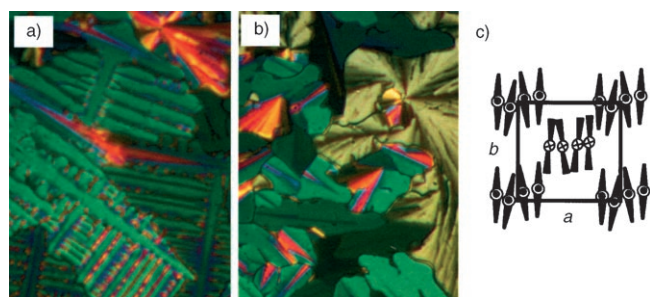


Figure 4. B1 mesophase of **En**. a), b) Optical photomicrographs (crossed polarizers) obtained at 144 °C. c) Possible model of the organization of compounds **En** in the B1 phase; the terminal chains (not shown) fill the space between the ribbons formed by the bend aromatic cores.

10°) dark and bright domains become visible (see Figure 6a). If the analyzer is rotated into the opposite direction the brightness of the domains is reversed (see Figure 6c), but the light transmission does not change if the sample is rotated.^[30] This indicates a conglomerate of macroscopically

chiral domains with opposite chirality sense. Hence, these mesophases show the typical features of “dark conglomerate phases”.

Up to now the precise structure of these “dark conglomerate phases” is not clear. The low birefringence could be explained with a SmC_aP_A phase structure with a 45° tilted organization of the molecules and a bending angle of the aromatic cores of about 109° (orthoconic anticlinic director structure)^[31,32] as recently proposed for a field-induced “dark-conglomerate phase”.^[23c] Also for compounds **Si1** and **Si2** the optically measured tilt angles (see Section on Field-induced textures) are in the range of 40–45°. However, in contrast to the field induced “dark conglomerate phase” reported in ref. [23c] these mesophases represent virgin structures, obtained without previous application of an electric field and hence their structure could be different. A low birefringent mesophase can alternatively result from a layer distortion which leads to a mesoscopically disordered structure, either composed of randomly ordered fragments of these layers,^[33] or due to a random (sponge-like) deforma-

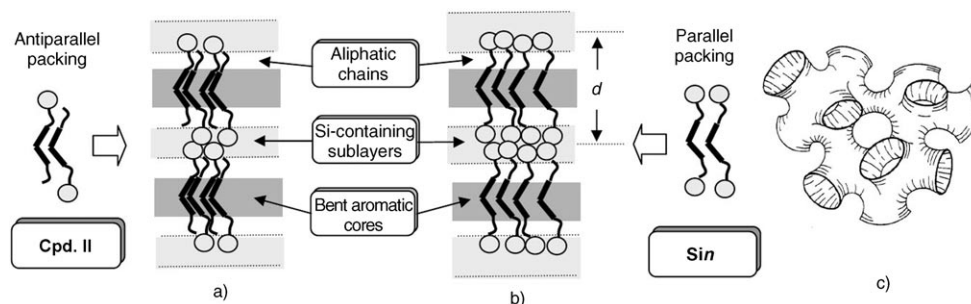


Figure 5. Models of the organization of the siloxane substituted bent-core molecules a) antiparallel packing of the monosilylated compounds **II**. b) Packing of the molecules **Si1** and **Si2** with silyl units at both ends as proposed for the arrangement of the molecules in the smectic phases (SmCP_{FE} , $\text{SmCP}_{\text{FE}}^{[*]}$ and SmCP_{A}) and in the ribbons of the Col_{ob} phases. c) Model of the sponge phase composed of deformed stacks of layers (only one layer is shown).

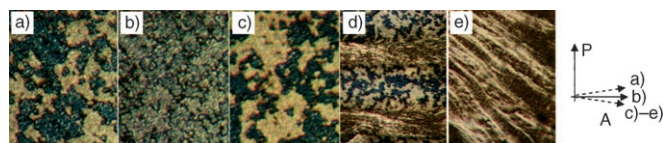


Figure 6. $\text{SmCP}_{\text{FE}}^{[*]}$ phase of compound **Si2** as seen at 150°C under a polarizing microscope a) between slightly uncrossed polarizers (arrows at the right indicate the positions of the polarizers in a)–e). b) Same region between crossed polarizers. c) Same region between slightly uncrossed polarizers, direction of the polarizers is reversed with respect to a). d) Coexistence of the conglomerate texture and oily streaks at the beginning of shearing; e) oily streaks and low birefringent schlieren-texture after completion of shearing.

tion of the layers.^[19f,34] In this case optical isotropy is independent of the tilt angle and it is possible for all polar smectic phases shown in Figure 2b if the size of the domains with uniform director orientation is smaller than the wave length of light. There are indeed strong arguments that the “dark conglomerate phases” of the silylated bent-core molecules represent smectic phases with a strongly folded and nonregular organization of the smectic layers, similar to sponge phases known from lyotropic systems (see Figure 5c).^[19f,34] At first, the layer reflections are not resolution limited and indicate a relatively short correlation length of the smectic layers. Secondly, in the absence of an electric field aligned samples could not be obtained for any of these smectic mesophases. Thirdly, the distorted structure is also obvious from the microscopic observation of the growing process, which is characterized by a fractal growing with a grainy and nonspecific appearance of the mesophase which is not typical for smectic phases with flat layers. Finally, in the case of a compound of type **II**, with a trisiloxane unit at only one end saddle-splay structures, confirming the sponge-like structure, were visualized by TEM of freeze-fracture samples.^[34] The typical properties of compounds **Si1** and **Si2**, seen in X-ray diffraction and optical experiments are very similar to those observed for related monosilylated bent-core molecules **II** and therefore a sponge-like distorted structure is assumed also for the “dark conglomerate phases” of these compounds. Moreover, the significantly higher viscosity of the mesophases of **Si1** and **Si2** in comparison to the convention-

al polar smectic phases of other bent-core molecules is also in line with the proposed sponge-like 3D organization.^[35]

As explained in the introduction, chirality in the polar smectic phases of achiral bent-core molecules arises from the tilted organization of the molecules in polar layers (see Figure 2). In the $\text{SmC}_{\text{a}}\text{P}_{\text{A}}$ and $\text{SmC}_{\text{s}}\text{P}_{\text{F}}$ phases the layers have identical chirality sense and hence, these structures are homogeneously chiral. Hough and Clark^[36] proposed that the optical activity of the “dark conglomerate phases” arises from this layer chirality.^[37] It requires the phase structure being homogeneously chiral and the birefringence of the mesophase itself is sufficiently small. This means that the “dark conglomerate phases” can either have an anticlinic and antiferroelectric $\text{SmC}_{\text{a}}\text{P}_{\text{A}}$ structure or a synclinic and ferroelectric $\text{SmC}_{\text{s}}\text{P}_{\text{F}}$ structure whereas the $\text{SmC}_{\text{s}}\text{P}_{\text{A}}$ and $\text{SmC}_{\text{a}}\text{P}_{\text{F}}$ phases are racemic and therefore optically inactive. Hence, only the kind of tilt correlation or the type of polar correlation should be known in order to assign the mesophase type, but this turned out to be very difficult. It is not possible to determine the layer correlation of the smectic phases under discussion by X-ray scattering experiments, because the distorted structure of these mesophases does not allow the growth of uniformly aligned samples for recording 2D diffraction patterns. Optical investigations also give no direct insight into the organization in the ground state, because well developed birefringent textures can only be obtained if the mesophases were grown under a DC electric field, which stabilizes the synpolar (FE) organization of the molecules. This means that the original mesophase structure is changed during investigation.

However, in the case of compounds **Si1** and **Si2**, in contrast to the related compounds **II** with only one silicon containing end group, shearing of the sample removes the chiral domains and gives rise to a birefringent texture with oily streaks and a schlieren texture between the streaks. The schlieren texture indicates an optically biaxial smectic phase, and the relatively low birefringence of the homeotropically aligned regions in the texture of **Si2** (see Figure 6e, regions between the stripes) suggests an anticlinic tilt correlation in this mesophase. This would be in favor of a $\text{SmC}_{\text{a}}\text{P}_{\text{A}}$ structure, if the classical models shown in Figure 2b are consid-

ered. However, the switching behavior is ferroelectric, which is in conflict with a classical SmC_aP_A phase structure as discussed on the basis of the results of electrooptical investigations in the next Section.

Electrooptical investigations of the smectic phases of compounds **Si1 and **Si2**:** Switching experiments in electric fields can give additional information concerning the organization of the molecules.^[14] The switching behavior under an applied triangular wave field and the optical observation of the textural changes in DC-field experiments are important tools.

Switching process under a triangular wave field: For the smectic phases of compounds **Si1** and **Si2** only one sharp single current response peak in the half period of a triangular-wave voltage was found over the whole mesomorphic temperature range (Figure 7a). The calculated polarization

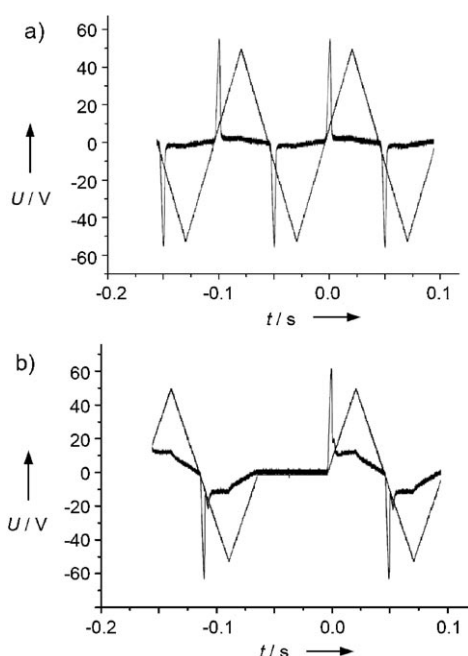


Figure 7. Switching current response of compound **Si1** in a noncoated $6\ \mu\text{m}$ ITO cell ($100\ \text{V}_{\text{pp}}$, $10\ \text{Hz}$, $5\ \text{k}\Omega$) on applying a) an alternating simple and b) modified triangular-wave voltage at $T=150^\circ\text{C}$. This type of curves can be observed over the whole temperature range of the mesophase between 65 and 150°C .

values are around $850\ \text{nCcm}^{-2}$. A modification of the triangular-wave field by a delay at zero voltage,^[38] using noncoated ITO cells,^[39] leaves the switching behavior unchanged, only one sharp peak is observed at all temperatures (Figure 7b). This means that immediately after zero voltage crossing a direct switching between the FE states with opposite polarity takes place and this is a strong indication of a bistable, that is, FE or FE-like switching process.

This FE switching suggests a synclinc SmC_sP_F structure (see Figure 8d) as a possible ground-state organization for the smectic phases of compounds **Si1** and **Si2**. However, this

synclinc organization would lead to a more birefringent schlieren texture in the shear-induced homeotropic regions (see Figure 6e). Investigations of carbosilane-derived bent-core mesogenic dimers^[19h] have shown that with increasing number of dimethylsilyl groups within the spacer units, there is a continuous transition from typical AF to surface-stabilized FE switching and it was proposed that this is due to a transition from an organization of alternating single layers (classical SmC_aP_A structure as shown in Figure 2b) to an alternating organization of stacks of synpolar layers.^[19h] Hence, a possible ground-state structure of compounds **Si1** and **Si2** could also be composed of SmC_sP_F clusters with a mesoscopic size. Figure 8c shows such a structure composed of SmC_sP_F layer stacks with an anticlinic and antipolar correlation between them ($[\text{SmC}_s\text{P}_F]_a\text{P}_A$ structure).^[40] This mesophase would have a low birefringence if the size of the SmC_sP_F layer stacks is sufficiently small. Because only the layer correlation of the interfaces between the layer stacks is changed during the switching process, and not the interfaces between each layer as in the classical models, a comparatively low voltage is required for switching. Hence, the FE states can be more easily stabilized by polar interactions with the substrate surface, leading to a bistable switching between the two surface stabilized FE states which give rise to only a single peak in the switching current curves. This means that the virgin ground-state structure could be overall AF and the actually observed switching is surface stabilized FE. In order to get additional information optical investigations of the switching process were carried out.

Field-induced textures: The textures of compounds **Si1** and **Si2** are significantly changed under the influence of external electric fields. Compound **Si1** will be discussed in more detail. For this compound, after application of an AC or DC field, the “dark conglomerate texture” becomes strongly birefringent and the chiral domains disappear. However, the textures obtained in this way are nonspecific. Well developed textures with circular domains were obtained on cooling **Si1** from the isotropic liquid state under an applied electric field above a certain threshold voltage. This means that under the electric field the sponge-like disordered layer structure of the ground state is unfolded and transformed into nondistorted layers.^[19,22] Because the layer polarization is parallel to the layer planes (along the bend-direction) the electric field, which is applied between the surfaces, induces a FE state with bookshelf geometry where the layers are perpendicular to the substrates. In the field induced circular domains the layers form concentric cylinders with the layer normal parallel to the substrates.

The actually observed type of circular domains depends on the characteristics of the electric field as well as on the applied voltage. Under a triangular wave AC field, independent of the voltage, exclusively low birefringent (grey) domains with extinction crosses parallel to polarizer and analyzer are formed (see Figure 10a). This indicates an anticlinic organization (either between single layers or between SmC_sP_F layer-stacks). The situation is different if a DC field

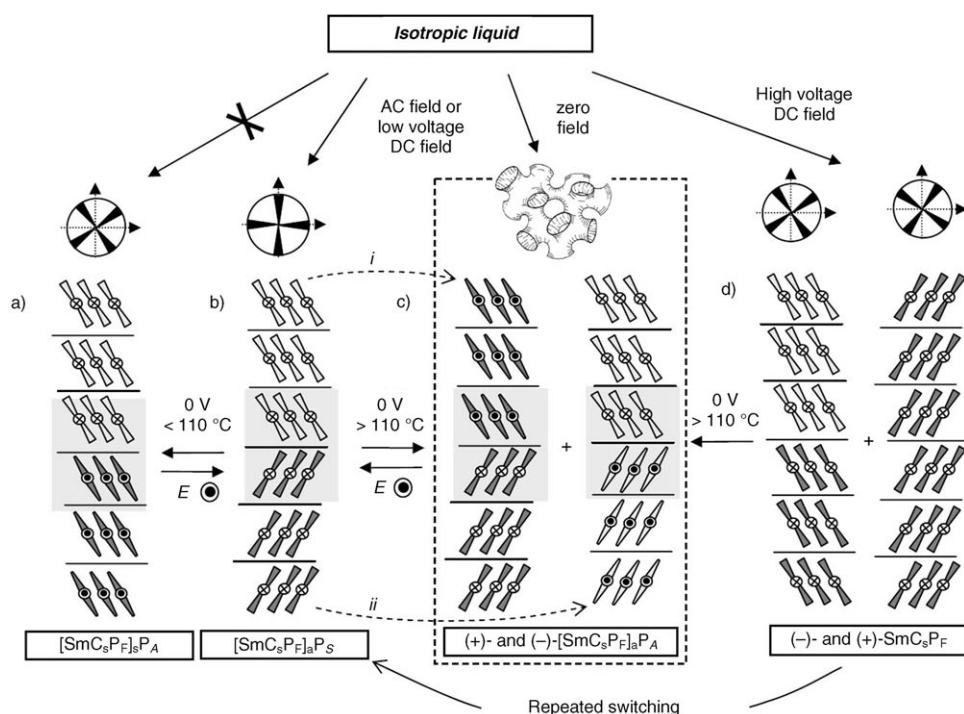


Figure 8. Proposed modes of organization of compound **Si1** depending on the conditions. The assignment of the phases is shown at the bottom, where the structure within the layer-stacks (SmC_sP_F) is given in square brackets and the following subscripts define the correlation of the interfaces between the layer-stacks (a = anticlinic, s = synclinic, A = antipolar, S = synpolar). a) Synclinic and antipolar $[\text{SmC}_s\text{P}_F]_s\text{P}_A$ structure as obtained in the relaxation process after switching off an applied AC voltage at $T < 110^\circ\text{C}$. b) Apparently anticlinic and synpolar $[\text{SmC}_s\text{P}_F]_a\text{P}_S$ structure as obtained by relaxation from structure b) and macroscopic chiral upon cooling from the isotropic liquid (dark conglomerate texture). c) Two enantiomeric $[\text{SmC}_s\text{P}_F]_a\text{P}_A$ structures as obtained either by cooling from the isotropic liquid state without applied field or in the relaxation process after switching off an applied AC voltage at $T > 110^\circ\text{C}$, it seems that the formation of this structure is associated with a layer deformation into a dark texture for which a sponge-like deformation of the layers is proposed; the chiral domains are microscopic in size (the phase appears optically inactive) if the phase is formed by relaxation from structure b) and macroscopic chiral upon cooling from the isotropic liquid (dark conglomerate texture). d) Uniform synclinic and synpolar SmC_sP_F structure as obtained upon cooling under a DC electric field with sufficient strength. The position of the extinction crosses with respect to the positions of polarizer and analyzer (arrows), as seen between crossed polarizers is shown at the top for each of the structures. The fundamental modes of organization shown in this Figure are also valid for the other compounds **Si2** and for **CSi3**.

is applied. Here the position of the extinction crosses additionally depends on the applied voltage. At low voltage ($0.5 \text{ V}\mu\text{m}^{-1}$) a low birefringent texture with coincident extinction crosses (as observed under an AC field) is formed exclusively. As the voltage is increased ($0.9 \text{ V}\mu\text{m}^{-1}$), few highly birefringent synclinic domains appear, where the extinction crosses are inclined with the positions of polarizer and analyzer. These synclinic domains become the majority at higher voltage and finally (at $3.5 \text{ V}\mu\text{m}^{-1}$) replace nearly all other domains (Figure 9a). Interestingly, the tilt angle of the extinction crosses is not uniform and once formed during the growing process under a certain voltage it cannot be modified by increasing the voltage.

The inclined position of the majority of dark extinction brushes obtained under a DC field (Figure 9a) indicates a field induced synpolar smectic phase with a predominately uniform tilt direction of the molecules in adjacent layers (SmC_sP_F phase). In the highly birefringent domains (e.g. domain A with blue birefringence color) the extinction

crosses are inclined with the directions of the polarizers by about $40\text{--}45^\circ$. Hence, the molecules in these domains seem to have $40\text{--}45^\circ$ tilted synclinic organization. However, there are many domains with lower birefringence which have extinction crosses with smaller angles (e.g. domain B)^[41] and also few very low birefringent domains with extinction crosses parallel to the directions of the polarizers (C) can be found. The occurrence of these quite different domains can be interpreted on the basis of a structure composed of SmC_sP_F layer stacks which are separated by anticlinic and synpolar interfaces (SmC_aP_F interfaces), as shown in Figure 8b. Here, the tilt direction changes between adjacent layer stacks. Due to the coupling of tilt direction and layer chirality, this structure can also be regarded as an alternating array of enantiomeric (+)- and (-)- SmC_sP_F layer stacks. If there is an equal number and size of the oppositely tilted SmC_sP_F stacks, and if the size of these stacks is smaller than the wave length of light, then the position of the extinction crosses coincides with the positions of polarizer and analyzer and the birefringence is low

(Figure 9a, domain C). This racemic structure is assigned as $[\text{SmC}_s\text{P}_F]_a\text{P}_S$.^[40] If there is a nonequal distribution of oppositely tilted (+)- and (-)- SmC_sP_F stacks, then, depending on their ratio, the extinction crosses can adopt different angles with respect to the polarizers (domain B). This structure, which is nonhomogeneously chiral is assigned as $(\mathcal{E})\text{-}[\text{SmC}_s\text{P}_F]_a\text{P}_S$, where (\mathcal{E}) indicates the configurational inhomogeneity of the system.^[42] If the uniform SmC_sP_F stacks have a macroscopic size, then the position of the extinction crosses becomes ca 45° inclined with the positions of the polarizers and synclinic domains (either (+)- or (-)- SmC_sP_F) can be observed (domain A).

This model is identical with a model proposed by Folcia et al.^[43] The authors suggest that the classical model of the SmC_aP_F structure, where polar layers strictly alternate (see Figure 2b) would be in conflict with the Curie principle and therefore a regular domain structure composed of alternating SmC_sP_F layer stacks was proposed for the field induced SmC_aP_F structure of bulk samples.

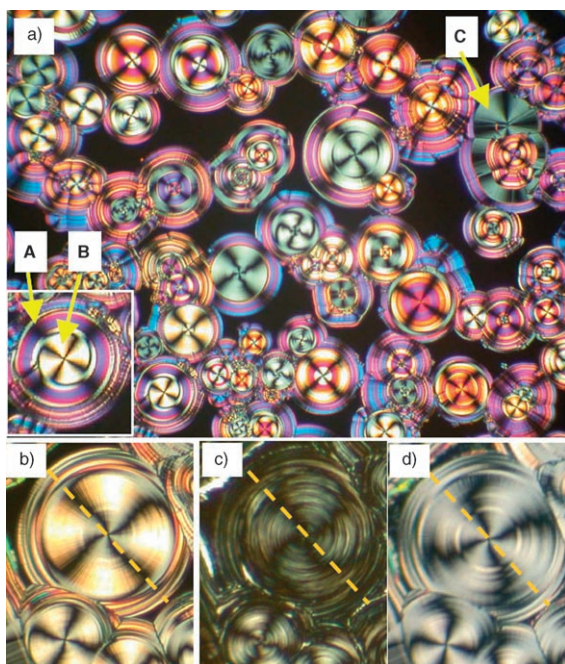


Figure 9. Field-induced textures of compound **Si1** as seen between crossed polarizers (polarizer and analyzer are positioned horizontally and vertically, respectively); a),b) ring-like circular domain structure after cooling the mesophase (1 K min^{-1}) under an applied DC field (12 V) at 158°C (noncoated ITO cells, $6 \mu\text{m}$); dark areas are residues of the isotropic liquid phase. c) Low birefringent texture as obtained after switching off the external electric field at 150°C . d) Texture as obtained after application of the electric field with opposite sign; the angle of the extinction crosses with respect to the position of the polarizers is changed as seen by comparison with the dotted line which indicates the initial position of the extinction crosses in b).

Under a stereochemical point of view the $[\text{SmC}_s\text{P}_F]_a\text{P}_S$ organization can be regarded as pseudoracemate, which is a racemic form between the conglomerates (SmC_sP_F and SmC_aP_A phases = association of uniformly chiral layers) and the racemic structures (SmC_sP_A and SmC_aP_F phases = association of layers with unlike chirality).^[20] This means that the energetic difference for the association of layers with the same or different chirality sense is relatively small. It seems that for the compounds under discussion the energetic difference between synclinal and anticlinal organization could indeed be rather small, due to the bulky Si-containing groups at both ends which can decouple the individual layers by the nearly isotropic oligosiloxane sublayers. Therefore, it is proposed that the SmC_sP_F structure is the preferred fundamental organization in the mesophases of the silylated bent-core molecules,^[19f] but also some anticlinal and/or antipolar interlayer interfaces coexist in a thermodynamic equilibrium. This gives rise to a variety of different textures. The growing of the mesophase under an electric DC field provides a preferred uniform tilt direction due to surface alignment, leading to a texture with predominately inclined extinction crosses. Depending on the strength of these alignment forces and the uniformity of the resulting domains, the observed extinction crosses can adopt different

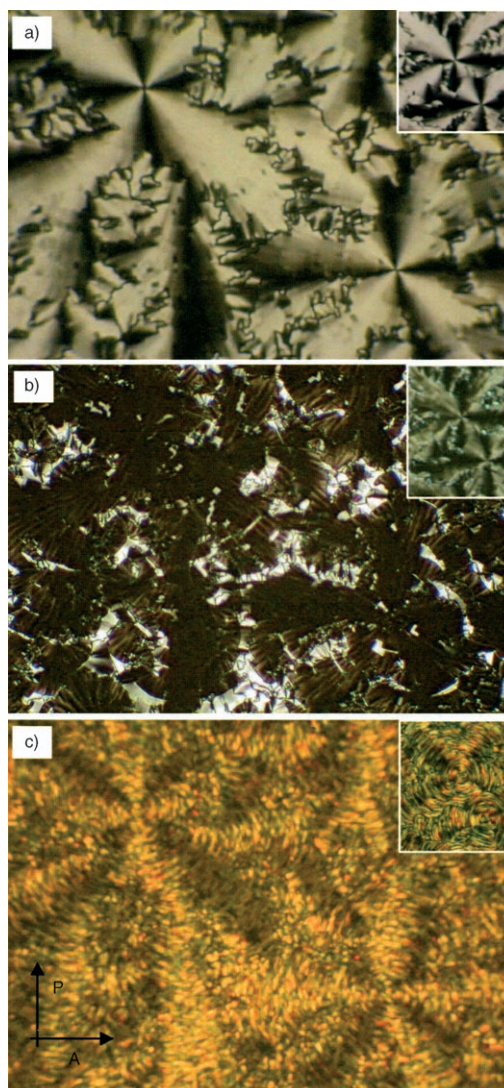


Figure 10. Textures of compound **Si1** as seen between crossed polarizers (polarizer and analyzer are positioned horizontally and vertically, respectively); a) low birefringent texture with apparently anticlinal domains as obtained under the applied AC field ($6 \mu\text{m}$ noncoated ITO cell, 100 V_{pp} , $f = 10 \text{ Hz}$) at all temperatures. b) Dark texture ca. 10 s after switching off the field at $T = 140^\circ\text{C}$. c) Highly birefringent texture characterized by synclinal domains ca. 10 s after switching off the field at $T = 80^\circ\text{C}$ (the brightness of a–c is scaled differently); application of an AC field to the textures shown in b) and c) immediately restores the texture a); the insets in a)–c) show the textures at the same temperatures, but in polyimide coated ITO cells ($6 \mu\text{m}$, 120 V_{pp} , $f = 100 \text{ Hz}$).

positions (see texture in Figure 9a). However, under a dynamic AC field a relatively large number of anticlinal layers is formed and this gives rise to a reduction of the size of the SmC_sP_F layer stacks and exclusively a low birefringent texture with extinction crosses parallel to the polarizers is observed (see Figure 10a).

Optical observation of the switching process: In a texture composed of predominately synclinal domains as obtained for **Si1** under a DC field (Figure 9b), switching off the ap-

plied DC field at 150°C distorts the circular domains. The overall birefringence is strongly reduced and some regions become completely isotropic. However, the position of the extinction crosses in the residual birefringent rings is not changed (see Figure 9c). Application of an electric DC field with opposite direction restores the birefringent circular domains, but the birefringence and the angle of the extinction crosses with respect to the polarizers are reduced in comparison to the starting situation (Figure 9d). This indicates that the field induced and surface stabilized synclinc structure is partly lost if the alignment field is removed. After several switching cycles (usually less than 10) all extinction crosses adopt positions completely parallel to polarizer and analyzer. A possible explanation could be that after removal of the external field a partial relaxation of the nearly uniform SmC_sP_F structure (see Figure 8d) to an antipolar and anticlinic $[\text{SmC}_s\text{P}_F]_a\text{P}_A$ structure (see Figure 8c) takes place by rotation on a cone. This locally polar structure (SmC_sP_F -layer stacks) adopts a sponge-like distorted structure which is optically isotropic and reduces the overall birefringence at 0 V. In addition, this relaxation seems to be irreversible and once the $[\text{SmC}_s\text{P}_F]_a\text{P}_A$ structure is formed it can only be switched into the corresponding synpolar and anticlinic domain structure ($[\text{SmC}_s\text{P}_F]_a\text{P}_S$, see Figure 8b) and this requires a rotation around the long axis. Hence, depending on the mesophase structure there are two distinct switching/relaxation processes. It also seems that the relaxation process does not take place in the whole sample. Whereas the uniform SmC_sP_F structure is retained at parts of the surfaces, there is a relaxation in the center of the sample. For this reason the position of the extinction crosses does not change after switching off the field, though the birefringence is reduced. After switching on the field again, the residues of the surface stabilized SmC_sP_F structure (inclined extinction crosses) and the field induced $[\text{SmC}_s\text{P}_F]_a\text{P}_S$ structure (coinciding extinction crosses) coexist and this gives rise to a reduced average angle of the extinction crosses with respect to the polarizers. Apparently, the number of uniformly tilted SmC_sP_F layers at the surface is reduced in each switching cycle and this leads to a reduction of the angle of the extinction crosses with respect to the polarizers until they coincide with polarizer and analyzer. At lower temperatures ($T < 110^\circ\text{C}$) the switching process becomes more complicated and highly birefringent domains occur beside the low birefringent domains.

In order to clarify the situation, temperature dependent electrooptical experiments were carried out with textures grown under an AC field in a noncoated 6 μm ITO cell. Under these conditions only extinction crosses coinciding with the positions of the polarizers were obtained (see Figure 10a, proposed structure is $[\text{SmC}_s\text{P}_F]_a\text{P}_S$). Depending on the temperature two slow relaxations to other textures can be observed. At temperatures above 110°C the dark extinction crosses do not change their position if the applied voltage is switched off, but the brightness of large areas of the texture significantly decreases (see Figure 10b) and in most regions the birefringent texture is completely replaced by

optical isotropic regions. The growth of the dark areas sets in immediately after switching off the field and, depending on the temperature and the frequency of the applied field,^[44] takes several seconds to minutes until the final completely dark state is reached. This type of optical response can be assigned to a relaxation of the surface stabilized FE and racemic $[\text{SmC}_s\text{P}_F]_a\text{P}_S$ structure (Figure 8b) into a disordered structure, which is macroscopically nonpolar and appears optically isotropic. It is assumed that the relaxation leads to an overall antiferroelectric $[\text{SmC}_s\text{P}_F]_a\text{P}_A$ structure (see Figure 8c) by a collective rotation of the molecules around their long axes. As shown in Figure 8b,c there is an equal probability of relaxation of the $(-)\text{-SmC}_s\text{P}_F$ layer stacks with formation of a $(+)\text{-}[\text{SmC}_s\text{P}_F]_a\text{P}_A$ structure (follow the dashed line i in Figure 8) and of $(+)\text{-SmC}_s\text{P}_F$ layer stacks with formation of a $(-)\text{-}[\text{SmC}_s\text{P}_F]_a\text{P}_A$ structure (follow the dashed line ii in Figure 8). Hence, the reorganization of the SmC_sP_F layer stacks into an overall AF structure leads to a macroscopically racemic mixture of microscopically chiral $(+)\text{-}$ and $(-)\text{-}(\text{SmC}_s\text{P}_F)_a\text{P}_A$ domains. This means that after relaxation, the overall structure should be similar to the virgin ground-state structure, that is, the flat layers are folded into a sponge-like structure, which is optically isotropic. However, no chiral domains could be detected, because the size of the uniformly chiral domains obtained after switching off the field is too small to be distinguished optically. It seems that macroscopic chiral domains ("dark conglomerate textures") are only formed by growing this mesophase from the isotropic liquid.

As the temperature is reduced, the dark regions formed after switching off the field become smaller, the relaxation process becomes slower and no change of the texture can be seen if the field is switched off at temperatures close to 110°C. It seems that at reduced temperature the more dense packing of the bent cores, coupled with an increased viscosity makes the rotation around the long axis more difficult. At $T < 110^\circ\text{C}$ another relaxation process is observed. At this temperature a slow transition to a strongly birefringent texture with extinction brushes inclined with polarizer and analyzer takes place in the zero-field state, indicating a transition to a purely synclinc phase structure (see Figure 10c).^[44] A relaxation of the $[\text{SmC}_s\text{P}_F]_a\text{P}_S$ phase (Figure 8b) into a $[\text{SmC}_s\text{P}_F]_s\text{P}_A$ structure^[40] shown in Figure 8a, with synclinc but antipolar boundaries is a possible mechanism of this relaxation. The $[\text{SmC}_s\text{P}_F]_s\text{P}_A$ structure is a macroscopically nonpolar (AF-like) and racemic structure. Reapplication of the electric field immediately restores the low birefringent texture with coincident extinction crosses (Figure 10a) as typical for the field induced $[\text{SmC}_s\text{P}_F]_a\text{P}_S$ phase (Figure 8b). This change of the orientation of the extinction crosses indicates that at this temperature the relaxation process should take place by rotation of the molecules on a cone.

Hence, the switching is surface stabilized FE at all temperatures. However, the FE states are metastable and after switching off the external field, two distinct relaxation processes to macroscopically nonpolar structures take place.

Depending on the temperature the relaxation process takes place either by collective rotation around the long axis or on a cone, which gives rise to the distinct appearance of the macroscopically nonpolar states. Because these relaxation processes are slow always only a single peak, resulting from the fast surface-stabilized FE switching process is found in the switching experiments under a triangular wave field. Furthermore, it seems that the formation of the sponge-like dark texture is only possible if the SmC_sP_F layer stacks adopt an anticlinic and antipolar correlation, that is, if the overall phase structure is homogeneously chiral. If an antipolar but synclinic structure, that is, a racemic structure is formed (at $T < 110^\circ\text{C}$) the birefringence is retained. For this reason, it seems that the formation of the dark conglomerate structure is bound either to a chiral superstructure or to the presence of some anticlinic interfaces.

Influence of surfaces: Switching in polyimide-coated measurement cells: It should be pointed out that surface interactions are of great importance for the actually observed switching behavior, and therefore any change of these surfaces can lead to different results. In polyimide-coated ITO cells, for example, no relaxation to a low birefringent texture can be observed at any temperature (see inset in Figure 10b), and the relaxation to the synclinic structure is also much slower. In addition, there is also an influence of these surface layers on the repolarization current curves. Only one switching current peak is observed under all conditions in ITO cells without additional coating layer. However, if polyimide-coated cells are used, the repolarization current curves are different. In these cells also a single peak is observed under a simple triangular wave field. However, under a modified triangular-wave field (when a delay is introduced at zero voltage) the single peak splits into two nearly identical peaks at high temperature, close to the clearing temperature. Upon reducing the temperature the two peaks become unequal in size and only at sufficiently low temperature a single peak is found (see Figure 11 a–c). This indicates that at high temperature the switching occurs around zero-voltage crossing^[45] whereas at low temperature switching occurs after sign reversal of the applied electric field (as observed in the noncoated cells at all temperatures).

The influence of the polyimide coating layer can be understood if it is considered that the internal electric field is influenced by the electric double layer formed at the surfaces. The field produced by this double layer is opposite to the applied external electric field, and hence, the internal field actually interacting with the LC is different from the applied (external) field (see Figure 12).^[46]

$$E = \frac{V - 2d'\epsilon' \sigma + P_0}{d + 2d'(\epsilon'/\epsilon)} \quad (1)$$

According to Equation (1) the strength of the resulting internal electric field (E) depends not only on cell thickness (d) and applied external voltage (V), but also on the thick-

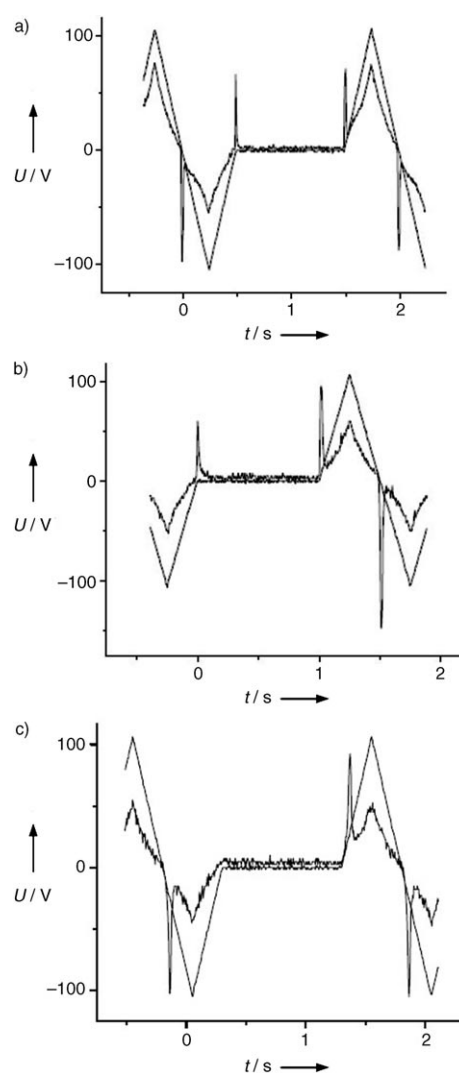


Figure 11. Switching current response curves of compound **Si1** in a 6 μm polyimide coated ITO cell ($\pm 105\text{ V}$, 1 Hz, 5 k Ω) on applying an alternating simple (regime of the downward current peak) and modified triangular-wave voltage (regime of the upward current peak/s) at a) $T = 140^\circ\text{C}$, b) $T = 85^\circ\text{C}$, c) $T = 65^\circ\text{C}$.

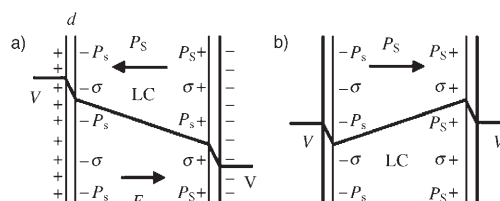


Figure 12. Influence of the electric double layer on the effective internal field (E) a) with applied external field and b) after switching off the external field.

ness (d') and the dielectric constant (ϵ') of the insulating alignment layer, on the related properties of the LC (d , ϵ) and on the surface density (δ) of ionic charges (P_0).^[46] Thus, the effect of the double layer is especially strong in ITO cells with an additional insulating polyimide alignment layer, if ionic impurities are present, and if the threshold

voltage of the switching process itself is low, as observed for many of the Si-containing bent-core molecules. Because the induced internal field is opposite in sign to the external field, the internal zero voltage is obtained before terminating the external field and the sign of the internal field is already reversed at zero external field (see Figure 12).^[46] If the threshold voltage (V_{th}) required for the switching process is smaller than the internally induced voltage (V_{int}), the switching process starts before crossing zero voltage ($V_{int} > V_{th}$). In this case the peak splits into two in a modified triangular wave field. The splitting is clearly visible at high temperature and gradually disappears on decreasing temperature as the threshold voltage increases at low temperature and V_{th} becomes larger than V_{int} . This explains why in the switching experiments with **Si1** in polyimide-coated ITO cells and at high temperatures no relaxation to a dark texture can be found upon terminating the field (see insets in Figure 10a,b). At zero external voltage the induced field switches some of the FE layers into the FE state with opposite polarity (peak before 0 V crossing). As switching takes place around the long axis, it does not change the texture, but it decreases the overall macroscopic polarity and this seems to reduce the driving force for the slow relaxation processes to the dark texture ($[SmC_sP_F]_aP_A$ structure). At reduced temperature the uniform polar structure is largely retained (only one peak after 0 V crossing) and a slow relaxation to the synclinc AF structure can be observed (see inset in Figure 10c). More generally, it is important to consider the effects of alignment layers in electrooptical investigations to exclude misinterpretations.

Electrooptical investigations of Si2: The switching behavior of the smectic phase of **Si2** is similar to that observed for **Si1**. For this compound, too, only one sharp current response peak in the half period of a triangular-wave voltage was found which only splits under a modified triangular wave voltage if polyimide coated ITO cells were used. Optical experiments show that the conglomerate texture is replaced by birefringent textures upon application of an electric field, but the textures are less well developed than in the case of **Si1**. The most obvious difference is seen in switching experiments, where, independent on the conditions, coinciding domains ($[SmC_sP_F]_aP_S$) always coexist with inclined (uniform SmC_sP_F) domains, indicating a stronger preference for a uniform synclinc organization. In addition, no relaxation can be observed in the anticlinic domains, neither to the dark texture, nor to highly birefringent synclinc domains. Only in the field induced synclinc domains some reduction of the birefringence is found after switching off the external field. It seems that the surface stabilization of the FE structure is more efficient and there is only some relaxation to the dark domain structure in the center of the sample.^[19] This means that the increase of the volume fraction of the silyl units stabilizes the uniform SmC_sP_F structure. The extinction crosses do not rotate, either by switching off the field or by applying the opposite field. This indicates a switching process which takes place by rotation

around the molecular long axis at all temperatures. This should be due to the additional space available between the bent aromatic cores, as a consequence of the more bulky silylated end groups in this compound.

Smectic and columnar phases of compounds **Si3**, **Si3i** and **CSi3**

Ground-state structures of Si3: Compound **Si3** with a trisiloxane unit shows a completely different and more complex behavior than **Si1** and **Si2** with smaller Si-containing units. On cooling from the isotropic liquid state the mesophase grows with a strongly birefringent texture containing sharp lines and leaf-like patterns and these features are indicative of a columnar phase. On further cooling, a phase transition can be observed at about 136 °C, which is seen by a significant decrease of the birefringence and viscosity (see Figure 13a,b). Upon heating this transition takes place at 143 °C (see Figure 13c). Hence, the high temperature phase can be significantly supercooled. On further cooling, at 126 °C there is an additional transition which is reversible and indicated only by a slight increase of the birefringence. At this temperature the switching-process changes from AF to FE (see next Section), but there is no clear peak in the DSC curves (Figure 13c) associated with this transition.

Over the whole mesomorphic region the two-dimensional X-ray diffraction pattern of an aligned sample shows two

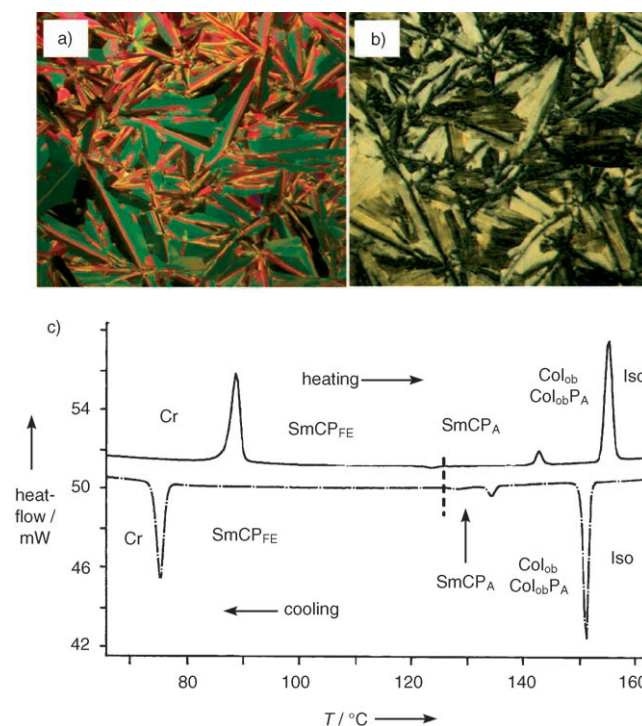


Figure 13. Optical photomicrographs (crossed polarizers) and DSC curves obtained for the mesophases of compound **Si3**: a) Col_{ob} phase at 149 °C, characterized by a strongly colored and highly birefringent texture. b) $SmCP_A$ phase as obtained on cooling the Col_{ob} phase to 130 °C, which represents a low birefringent grey texture. c) DSC traces (10 K min⁻¹, first heating- and cooling runs).

diffuse maxima in the wide-angle region (see Figure 14a,b,d,e). The diffuse character of these reflections confirms the LC character of the mesophases. The diffuse maximum at about 0.47 nm, corresponding to the mean distance within the aromatic/aliphatic parts, is split of into two crescent-like halos in the 2D diffraction patterns of an aligned sample. These diffuse halos are inclined with meridian and equator which indicates a tilted organization of the molecules with a tilt angle of about 45°. At high temperature ($T > 143^\circ\text{C}$), the intensity of both maxima is different (see Figure 14b, and Figure S2d, Supporting Information, thick black line), which most probably arises from a synclinal tilt of the molecules, whereas below 143°C the intensity becomes nearly equal (Figure 14e, and Figure S2d, Supporting Information, thick red line) which is in line with a transition to a mesophase with an anticlinic tilt organization, as also identified in optical experiments (see below). In the whole mesomorphic range the inner diffuse scattering corresponding to a mean distance of $d=0.70$ nm shows that the siloxane units are segregated and form distinct sublayers. Within these layers the siloxane units are strongly disordered as indicated by the nearly ring-like shape of this scattering (see Figure 14a,d). There is only a slightly reduced intensity of this scattering around and at the meridian (see intensity distribution along χ shown in Figure S2d, Supporting Information).

The small angle scattering also changes with temperature. At $T > 143^\circ\text{C}$ the X-ray diffraction pattern (Figure 14c) shows reflections positioned on the meridian as well as out of equator and meridian, which indicate a columnar mesophase. These reflections can be indexed to an oblique lattice with the lattice parameters, $a=5.8$, $b=5.1$ nm and $\gamma=114.5^\circ$ (see Table S1, Figure S3g, Supporting Information). Accordingly, this mesophase is a modulated smectic phase with oblique 2D lattice, where the smectic layers are fragmented into ribbons (ribbon phase). The lattice parameter a corresponds to the width of the ribbons (ca. 6–7 molecules per unit cell, that is, there are about 6–7 molecules in the cross-section of each ribbon, see Table S2, Supporting Information) and b compares to the thickness of the ribbons. The value $b=5.1$ nm is less than the calculated molecular length ($l=7.2$ nm), which is due to the significant tilt of the molecules with respect to the direction b . Because of this 2D lattice the phase is assigned as Col_{ob} . In electrooptical experiments (see the next section) at higher tem-

perature ($T > 147^\circ\text{C}$) this phase does not show any response on an applied electric field (Col_{ob}), whereas at lower temperature an AF switching process was found ($\text{Col}_{\text{ob}}\text{P}_A$). The inset of polar order is not associated with any change in the X-ray diffraction pattern and it also cannot be detected in the DSC traces.

At 143°C , at the transition from the columnar phase to the low temperature phase,^[47] the cross reflections corresponding to the 2D lattice completely disappear and only layer reflections ($d=4.8$ nm at 120°C) are retained as shown in Figure 14d,f, which indicate the smectic nature of this mesophase. From the position of the wide angle reflections a tilted organization (tilt angle of ca. 45°) can be concluded. The diffraction pattern does not significantly change by further reduction of the temperature until crystallization occurs. In the smectic phases the layer reflections are unusually broad (see Figure 14f). This would be in line with an undulated smectic phase and in the case of the isomeric compound **Si3i** the undulated structure was additionally confirmed by the observation of satellites occurring beside these layer reflections.^[16] For compound **Si3**, however, based on X-ray data, there is no unambiguous proof of a layer undulation because at the transition from the columnar to the smectic phase the uniform alignment obtained in the columnar phase is partially lost so that any extension of the layer reflections parallel to the equator would be overlapping with a broadening of these reflections due to multidomain formation. For this reason there is also no clear difference seen in the shape of the layer reflections at the temperature where the switching changes from AF to surface stabilized FE (see next Section). These smectic mesophases are assigned as SmCP_A and SmCP_{FE} , respectively.

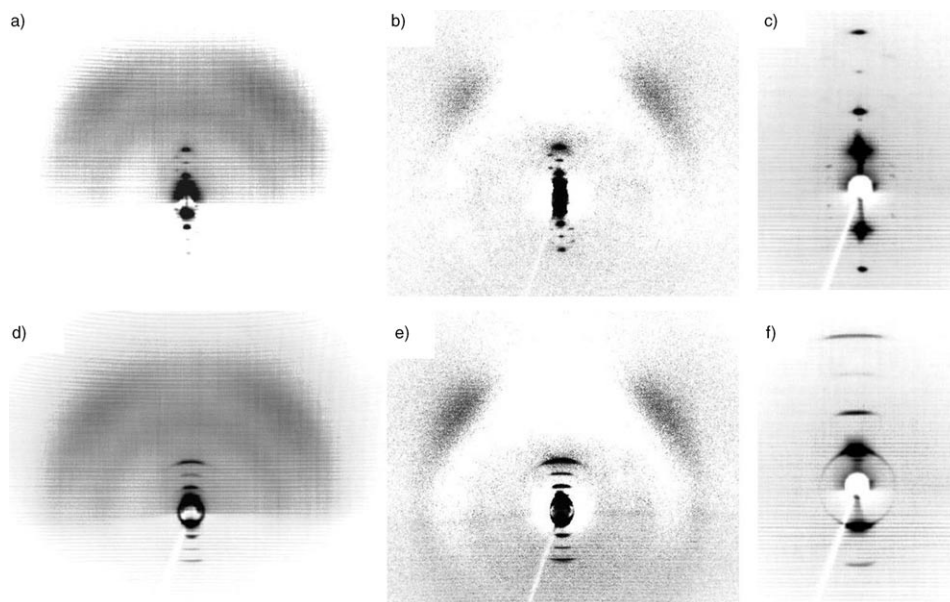


Figure 14. Two-dimensional X-ray diffraction patterns of an aligned sample of compound **Si3** at 148°C a)–c) and at 120°C d)–f), on cooling: a), d) original patterns, b), e) the scattering of the isotropic liquid subtracted from the original patterns to enhance the effect of the nonisotropic distribution of the outer diffuse scattering, c), f) reflections in the small-angle region, see also Table S1 and Figure S3, Supporting Information.

The smectic phases (SmCP_A and SmCP_{FE}) possess schlieren textures with relatively low birefringence, the same as obtained for **Si2** after shearing. Remarkably, there is no formation of a chiral or nonchiral dark texture upon cooling from the $\text{Col}_{ob}P_A$ phase. It seems that an optically isotropic (sponge-like) phase cannot be formed upon cooling from a columnar (modulated smectic) phase. Nevertheless, there seems to be an inherent tendency for layer deformation and layer distortion in these smectic phases as in X-ray experiments, at the transition from the columnar to the smectic phases, the well aligned samples of the columnar phases always irreversibly lose their alignment.

Electrooptical investigations of Si3: On cooling the isotropic liquid under a triangular-wave electric field of about ± 105 V ($6 \mu\text{m}$) at a frequency of 10 Hz the columnar phase appears with a mosaic-like texture, but no polarization current response can be observed, as shown in Figure 15a. The textural pattern obtained under these conditions is indistinguishable from the natural texture of this mesophase and indicates that the mesophase structure is not influenced by the field. In this texture, domains in which the ribbons are aligned parallel or perpendicular to the analyzers are bright, whereas those which are inclined with the positions of the polarizers are dark and this confirms a synclinal tilted organization in this mesophase. The absence of a polarization current response confirms the missing long range polar order. That means that the rotation of the molecules around the long axis is nearly free. This is feasible as there is sufficient space provided for the bent cores by the bulky heptamethyltrisiloxane units at both terminal positions.

Upon cooling, below 147°C , that is, in the temperature region of the $\text{Col}_{ob}P_A$ phase two polarization current peaks appear, accompanied by a textural change as shown in Figure 15b. The two peaks in each half period of the applied triangular wave voltage indicate an AF switching process ($P_s = 300 \text{ nC cm}^{-2}$ at 140°C) between 147 and 136°C (transition temperature to the smectic phase on cooling). The dark areas within the texture remain at the same position, which means that the tilt remains synclinal. The synclinal tilt is further confirmed by DC field experiments where the extinction crosses in circular domains are inclined with the positions of polarizer and analyzer (see inset in Figure 15b). In addition, no change of the position of the extinction crosses can be seen either by removing the field or by reversing the field (see Figure S4a–c, Supporting Information). This indicates that the AF switching process takes place by an elastic rotation of domains around the long axes. It seems that at reduced temperature, within the temperature range of the columnar phase, due to the reduced space required by the end-groups a polarization along the bent direction results, leading to an inset of polar order. In this $\text{Col}_{ob}P_A$ phase the switching process takes place by collective rotation around the long axis and the polarization values observed in this phase are relatively small.

On further cooling, at the transition to the smectic phase at 136°C , the birefringence drops and the dark and bright

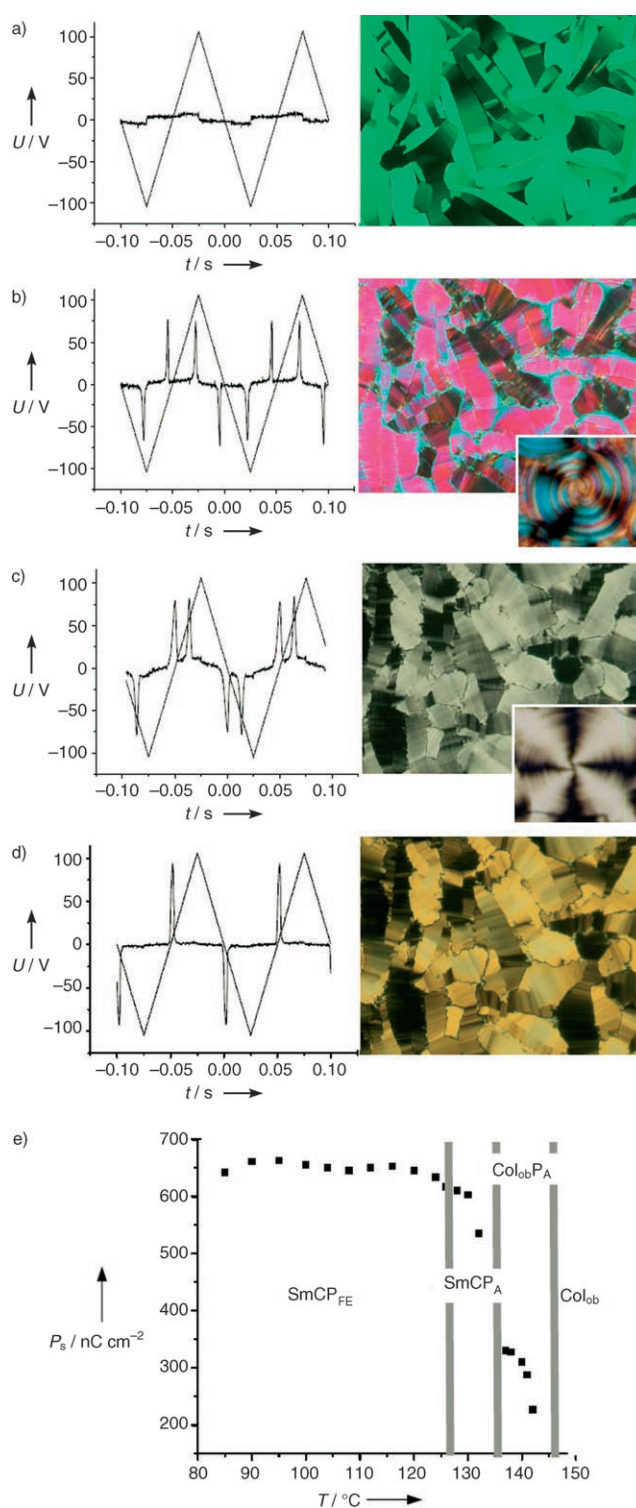


Figure 15. Switching current response traces (left) obtained under a triangular-wave field (± 105 V, 10 Hz, $6 \mu\text{m}$ polyimide coated ITO cell) and the corresponding textures (right) of the mesophases of compound **Si3** a) Col_{ob} phase at 148°C . b) $\text{Col}_{ob}P_A$ phase at 144°C . c) SmCP_A phase at 130°C . d) SmCP_{FE} phase at 100°C . e) Plot of the spontaneous polarization of the mesophases of compound **Si3** depending on the temperature.

areas in the texture are exchanged (Figure 15c). Also, in the circular domains the extinction crosses rotate to positions

coincident with the polarizers (compare insets in Figure 15b,c). This indicates a transition from the synclinc organization to an organization with an alternating tilt-direction either between the individual layers (SmC_aP_F , see Figure 2b) or between stacks of synclinc layers ($[\text{SmC}_s\text{P}_F]_a\text{P}_S$ structure, see Figure 8b). The AF switching behavior is retained at this phase transition but the position of the repolarization current peaks is changed. The two widely separated peaks, seen in the $\text{Col}_{\text{ob}}\text{P}_A$ phase, disappear and two closer peaks appear in the smectic phase (in the two phase range all four repolarization peaks can be observed, see Figure S5, Supporting Information). This indicates that the energy difference between the two FE states and the AF ground-state structure is reduced. Also in the temperature range of the smectic phase the position of the extinction crosses does not change during the switching process. Hence, though the phase structure is changed, the AF switching still takes place by rotation around the long axis. In addition, a strong increase in the polarization value is observed at this transition. The polarization value saturates at $P_s = 650 \text{ nC cm}^{-2}$ with further decreasing temperature (see Figure 15e).

At 126°C one of the polarization peaks (that one occurring at higher voltage) disappears, indicating a transition to a FE switching process (Figure 15d). This transition cannot be observed by X-ray diffraction or DSC (see Figure 13c), but in the field induced textures, a slight increase of the birefringence can be seen (compare Figure 15c and d). The field induced circular domains which coincide with the directions of the polarizers do not change their position at this temperature, and during switching no change of the position of the extinction crosses can be found (see Figure S4d–f, Supporting Information). This means that at 126°C the stability of the FE states is further increased and causes a FE switching which also takes place as a collective rotation around the long axis. It seems that at this temperature the surface stabilization of the more polar FE structure becomes dominating, leading to a surface stabilized FE switching, similar to that observed for compounds **Si1** and **Si2**.

Dielectric investigations: Dielectric investigations were carried out with a much lower external electrical voltage. Therefore, the orientation of the molecules and the structure of the phases are not disturbed. This method is sensitive to changes in the short range order within the mesophases. Data of compound **Si3** (Figure 16) indicate two main relaxation processes, one associated with the fast rotation of the molecules around the long axis (f_{R2}) and the second one at lower frequency is a collective process (f_{R1}). The complex fit of the raw data to two Cole–Cole mechanisms, conductivity and electric double layer results in the limits of the dielectric permittivities ϵ_0 – ϵ_2 and the related relaxation frequencies f_R at different temperatures.^[48] As seen in Figure 16a, there is a strong temperature dependence of the relaxation frequency f_{R2} . The rotation of the molecules is very fast in the isotropic phase (it cannot be seen in our time window), decreases stepwise at the Iso– Col_{ob} transition and becomes significantly slower in the temperature range of the Col_{ob}

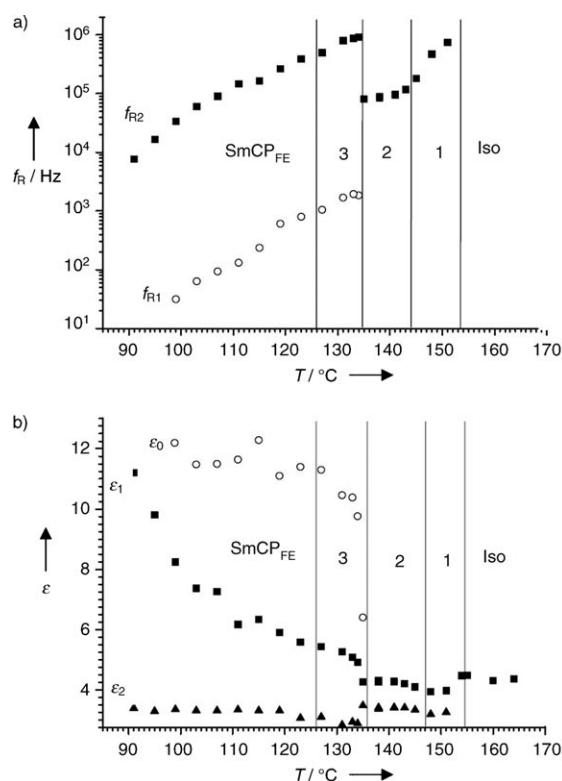


Figure 16. a) Relaxation frequencies and b) limits of the dielectric permittivities as obtained for compound **Si3** from the fit to two Cole–Cole equations as described in ref. ^[48] The phase transitions are indicated as vertical lines. Phase regions: 1 = Col_{ob} , 2 = $\text{Col}_{\text{ob}}\text{P}_A$, 3 = SmCP_A .

phase with decreasing temperature until the onset of polar order (transition to $\text{Col}_{\text{ob}}\text{P}_A$). This is in line with the proposed model for the Col_{ob} to $\text{Col}_{\text{ob}}\text{P}_A$ transition (see preceding section). In this temperature range the effects in the dielectric permittivity ϵ_1 are low and hence it is experimentally difficult to separate the small low frequency relaxation from the conductivity. The picture changes dramatically at the $\text{Col}_{\text{ob}}\text{P}_A$ to SmCP_A transition. The stepwise increase of f_{R2} at this transition is associated with the transition from a ribbon structure, where the inter-ribbon boundaries restrict the rotation, to infinite layers where the rotation around the molecular long axis is less hindered. From the decrease of f_{R2} with temperatures in the smectic phases an activation energy of 56 kJ mol^{-1} was calculated for the rotation around the long axis. Furthermore, a pronounced low frequency absorption appears. Remarkably, there is no visible change of f_{R1} and f_{R2} at 126°C where the transition from AF to FE switching is observed in electrooptical experiments. The dependence of the dielectric constants ϵ on the temperature is shown in Figure 16b. The most remarkable feature seen in Figure 16b is the strong increase of the dielectric permittivities ϵ_1 and ϵ_0 at the transition from the columnar to the smectic phases, whereas no significant change can be observed at the transitions Col_{ob} to $\text{Col}_{\text{ob}}\text{P}_A$ and SmCP_A to SmCP_{FE} . This indicates that the positive dipole coupling is strongly enhanced at the transition from the columnar to

the smectic phase, whereas no significant change takes place at the transition from AF to FE switching in the smectic phase region. This observation confirms the proposed organization of the molecules in these smectic phases. The high dielectric permittivities of the low frequency limit ϵ_0 indicate a positive coupling of the molecular dipole moments in large clusters. Also the high values of the dielectric permittivities ϵ_1 in the SmCP_A phase cannot be satisfactorily explained with a SmC_aP_A structure where the polar direction changes from layer to layer. It is more in line with the proposed organization of the molecules in alternating SmC_sP_F layer stacks ($[\text{SmC}_s\text{P}_F]_a\text{P}_A$ structure, see Figure 8c). In the temperature range of the SmCP_A phase there is a relatively strong increase of ϵ_0 with decreasing temperature which should be due to a decrease of rotational disorder of the molecules with temperature. This is also related to the significant increase of the spontaneous polarization from about 300 nCcm^{-2} at the $\text{Col}_{\text{ob}}\text{P}_A$ to SmCP_A transition to about 600 nCcm^{-2} at the SmCP_A to SmCP_{FE} transition (see Figure 15e) and the further increase within the SmCP_{FE} phase. It seems that at the SmCP_A to SmCP_{FE} transition at about 126°C a sufficiently dense packing of the molecules is achieved which enhances the polarization and allows a coupling of these polar layer stacks to the polar cell surfaces. This stabilizes a uniform SmC_sP_F structure also at zero voltage, which is seen as a transition from AF to surface stabilized FE switching. Accordingly, there is no change of the fundamental phase structure at the AF to FE transition; there is only a reduction of the degree of rotational disorder due to the changing packing density of the bent-core units. The slight increase of the birefringence at the transition to the SmCP_{FE} phases (see Figure 15c,d) might also be due to the increase of polar order.

The mesophases of Si3i: Compound **Si3i** which has branched heptamethyltrisiloxane units instead of the linear ones in **Si3** was reported earlier.^[16] This compound has also a $\text{Col}_{\text{ob}}\text{P}_A$ high temperature phase ($a=2.5$, $b=4.65 \text{ nm}$; $\gamma=107^\circ$)^[28] and a smectic phase (USmCP_A) at lower temperature. As reported for **Si3** there is a transition from a synclinc organization in the $\text{Col}_{\text{ob}}\text{P}_A$ phase to an apparently anticlinic organization in the smectic phase, a change of the position of the repolarization current peaks at the phase transition, and the switching takes place by rotation around the long axis in both mesophases. Hence, the branched compound **Si3i** is similar to the isomeric nonbranched compound **Si3**, but there are also differences. Namely, the size of the ribbons in the $\text{Col}_{\text{ob}}\text{P}_A$ phase of **Si3i** is much smaller than in the $\text{Col}_{\text{ob}}\text{P}_A$ phase of **Si3**.^[28] Only 2–3 molecules are organized in the cross-section of these ribbons. In contrast to **Si3** the switching is AF over the whole temperature range of the columnar and the smectic phases, that is, there is no transition to a FE switching phase at low temperature and no loss of the polar order at high temperature. The smaller size of the ribbons in the $\text{Col}_{\text{ob}}\text{P}_A$ phase seems to compensate the larger effective size of the branched heptamethyltrisiloxane units with respect to the linear ones. The stronger

layer distortion by these branched end-chains seems also to be responsible for the maintenance of AF switching at lower temperature (see explanation given in Section on Effects on the switching process).

The mesophases of CSi3: The carbosilane derivative **CSi3** also behaves similar to **Si3** (see Table 1). There is a high temperature $\text{Col}_{\text{ob}}\text{P}_A$ phase which is replaced at lower temperature by two smectic phases with apparently anticlinic organization. There is a change of the position of the repolarization current peaks at the transition from the columnar to the smectic phase and in the temperature region of this smectic phase there is a transition from AF to FE switching at 132°C (see Figure S6a–c, Supporting Information).^[49] The switching takes place around the long axis in the whole mesomorphic temperature range. In contrast to **Si3**, but similar to **Si3i** AF switching is found over the whole temperature range of the $\text{Col}_{\text{ob}}\text{P}_A$ phase ($\text{Col}_{\text{ob}}\text{P}_A$). However, the textures are less specific (see Figure S7, Supporting Information) and for X-ray scattering no well aligned samples of the mesophases have been obtained. Only one very weak nonlayer reflection has been found in the X-ray diffraction pattern of the columnar phase (see Figure S8, Supporting Information). The assignment of these reflections to a distinct oblique lattice ($a=2.8$, $b=5.1 \text{ nm}$, see Table 1 and Table S1, Supporting Information) is more or less tentative and done in analogy to the corresponding phases of **Si3** and **Si3i**. Furthermore, in the field aligned samples no clear textural changes take place at the $\text{Col}_{\text{ob}}\text{P}_A$ to SmCP_A transition and in the temperature range of the $\text{Col}_{\text{ob}}\text{P}_A$ phase the synclinc domains formed by cooling under a DC field (or by cooling without applied field) are replaced by apparently anticlinic domains under a triangular wave voltage, as typically observed for the smectic phases of **Si1** and **Si2**. It seems that in the case of compound **CSi3** the alignment field can easily remove the layer modulation of the $\text{Col}_{\text{ob}}\text{P}_A$ phase which would require a synclinc tilt.

Conclusions

The development of the mesophases in the series of compounds **Si1–Si3**, **CSi3** and other silicon containing bent-core molecules should mainly result from two competitive forces provided by the silyl units, namely layer decoupling and steric frustration.

The effect of layer decoupling on the structure of the smectic phases

Ferroelectric versus antiferroelectric switching: An important effect of the Si-containing units is their tendency to segregate into distinct isotropic sublayers which decouple the layers of the bent-core units. This effect increases with elongation of the silylated units and it has a large impact upon switching behavior and interlayer correlation. Usually, the AF organization in the liquid crystalline phases of bent-core

molecules allows an easy fluctuation of the molecules from layer to layer, because the wings of the bent cores are organized in a synclinc fashion at the inter-layer interfaces (see Figure 17a). These fluctuations, which stabilize the AF

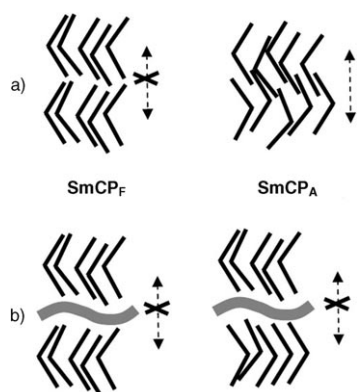


Figure 17. Effect of segregated siloxane sublayers upon the out-of-plane interlayer fluctuations (dashed arrows) in the SmCP_A and SmCP_F phases of a) conventional bent-core molecules of type I (see Figure 3) and b) bent-core mesogens with micro segregated siloxane or carbosilane sublayers (compounds **Sin**, **CSi3**, **II** and **III**); these sublayers suppress the fluctuations and therefore reduce the entropic penalty of the SmCP_F organization with respect to the SmCP_A structure.

organization entropically, are more difficult in the FE structures, where the wings of the bent cores are organized in an anticlinic fashion at these interfaces and hence disturb these fluctuations. This leads to an entropic penalty for the FE structure which is especially strong for conventional banana molecules with linear alkyl chains. Branching of the alkyl chains^[15a-c,h,l] or any other structural change at the ends of these chains, which reduces the conformational order at the interlayer interfaces reduces these fluctuations, reduces the entropic penalty for the FE structure and makes the FE structure more favorable (see Figure 17b). The nearly isotropic siloxane sublayers are especially effective in this respect and after alignment in an electric field, surface stabilized FE switching is observed for most of the smectic phases of the silylated compounds.^[19] On the other hand, interactions between the chain ends can stabilize the FE structure of alkyl substituted molecules energetically,^[50] but this effect is assumed to be less important for the siloxane derivatives, due to the disordered (nearly isotropic) character of the oligosiloxane sublayers which are located at the interlayer interfaces. Therefore, the virgin ground-state structure of the silylated bent-core molecules should be overall AF, but FE states can easily be achieved by surface stabilization.^[51] In order to distinguish these surface stabilized FE switching mesophases from those with virgin FE ground-state structures (polarization modulated SmC_sP_F phases^[52] or SmC_aP_F phases^[15b,c,l] with polarization splay between the cell surfaces^[53,15c]), these mesophases are assigned as $\text{SmCP}_{FE}/\text{SmCP}_{FE}^{[*]}$, as suggested recently.^[13c] In this notation the subscript “FE” indicates the experimentally observed switching behavior and not the mesophase structure in the ground

state which is actually $[\text{SmC}_s\text{P}_F]_a\text{P}_A$ for the compounds under discussion.

From the experimental results it seems that there is some preference for a synclinc tilted and synpolar (FE) organization in the mesophases of these silylated compounds. Hence, the fundamental phase structure is SmC_sP_F , but as the layers are strongly decoupled by the Si-containing sublayers, there seems to be a relatively low energy difference between synclinc and anticlinic organization and therefore some anticlinic interfaces can coexist in a thermodynamic equilibrium with the synclinc correlated layers. Depending on the precise molecular structure and the experimental conditions, the size of the SmC_sP_F layer stacks could be different, which leads to distinct types of switching current response curves. With increasing size of the SmC_sP_F layer stacks the switching process changes from classical AF (two well separated peaks, switching of relatively thin SmC_sP_F layer stacks) via single-peak-AF (single peak at 0 V crossing, switching of larger SmC_sP_F layer stacks^[19h]) to surface stabilized FE (single peak after 0 V crossing, switching between surface stabilized macroscopically polar SmC_sP_F structures).

Surface alignment forces can also stabilize a uniform synclinc organization during growth of the phase from the isotropic liquid state under a static electric field (DC field). The ring-like appearance of the synclinc domains obtained under these conditions can be explained by the presence of synpolar and anticlinic SmC_aP_S interfaces in these field induced samples ($[\text{SmC}_s\text{P}_F]_a\text{P}_S$ structure). If the concentration of anticlinic defect-layers is sufficiently high that the size of the synclinc stacks of the layers becomes smaller than the wave length of light, then only an average optical axis parallel to the layer normal is seen. This gives rise to a low birefringent texture with extinction crosses coinciding with the directions of the polarizers as seen for the mesophases grown under a dynamic AC field. If an unequal number of differently tilted layers are combined, the extinction crosses adopt an angle which is intermediate between these two cases.

“Dark conglomerate” versus birefringent mesophases:

Though the $[\text{SmC}_s\text{P}_F]_a\text{P}_A$ ground-state structure is macroscopically nonpolar, there is a local polarity within the SmC_sP_F layer stacks which can be minimized by a splay of these layers, producing a sponge-like structure. The decoupling of the layers by the siloxane sublayers and the steric frustration arising from the space required by the silyl units can additionally contribute to the destabilization of flat layers and supports layer deformation.

Remarkably, the $[\text{SmC}_s\text{P}_F]_s\text{P}_A$ structure (Figure 8a) does not relax into the dark texture, whereas the $[\text{SmC}_s\text{P}_F]_a\text{P}_A$ structure often does, and this suggests that anticlinic interfaces are important for the formation of these dark phases. It is known that these anticlinic layers disfavor a regular 2D modulation of the SmC_sP_F layers into polarization modulated smectic phases (B7-type mesophases). Hence, it is suggested that the formation of sponge-like disordered phases is an alternative way for SmC_sP_F structures to escape from a

(mesoscopic) polar order if anticlinic defect layers cannot be suppressed. The $[\text{SmC}_s\text{P}_F]_a\text{P}_A$ structure is homogeneously chiral and the optical activity of this mesophase can be detected as regions with uniform optical rotation. The chirality can easily be observed, because the sponge-like structure itself is optically isotropic.^[36] These sponge-like structures represent random 3D-networks of layers and therefore a portion of the molecules is always in direct contact with the substrate surfaces. For this reason, surface alignment effects can fix the chirality sense once established in the growing process over macroscopic regions, leading to a stable structure composed of domains with opposite chirality sense. Depending on the number of layers within the SmC_sP_F stacks and the degree of polar order within the layers, the layer distorting force, that is, the desire to escape from mesoscale polar order, can have different strength. Hence, the “dark conglomerate texture” can be very robust as observed for most monosilylated compounds of type **II**. For compounds **Si1** and **Si2**, however, this texture is less stable and can be disrupted by mechanical shear forces, which lead to birefringent textures.

As also the switching behavior is dependent on size and polarity of the SmC_sP_F layer stacks (see previous Section) “dark conglomerate phases” can show either FE or non-classical types of AF switching (single peak at 0 V or two relatively close peaks).^[13b] Only if the size and polarity of the layer stacks is below a certain critical value, then the driving force for layer distortion is too small. In this case exclusively birefringent textures and classical AF switching behavior (two well separated peaks) can be observed (B2 phases).

It is also remarkable that the birefringent textures obtained after mechanical shearing of **Si1** and **Si2** do not spontaneously reorganize to the sponge-like structure, whereas this structure is immediately formed from the field induced $[\text{SmC}_s\text{P}_F]_a\text{P}_S$ structure after removal of the alignment field (see the section on optical observation of the switching process). A possible explanation could be that in the field induced structure there are relatively large uniformly aligned polar regions (ferroelectric clusters) which provide a strong driving force for layer distortion. In the sheared samples the FE clusters could be much smaller and hence, there might be a weaker driving force for layer distortion.

If there are exclusively SmC_aP_A type defect layers the SmC_sP_F layer-stacks have a uniform chirality sense and the macroscopic chiral domains can be observed optically (“dark conglomerate phases”). If there are additional SmC_aP_S interfaces, or if (+)- and (-)- $[\text{SmC}_s\text{P}_F]_s\text{P}_A$ structures are mixed, then the chiral domains cannot be distinguished optically and low birefringent textures without chiral domains can be observed.^[19i,33] Such textures were observed for compound **Si1** after switching off the AC field at $T > 110^\circ\text{C}$, for carbosilane based dendrimers with bent-core units^[19j] and occasionally also in the smectic phases occurring below nematic phases of bent-core molecules.^[33]

Hence, the proposed models can satisfactorily explain the experimental findings associated with the occurrence of

these optically isotropic mesophases of bent-core molecules. Moreover, it seems that beside the four classical structures shown in Figure 2b there is a broad spectrum of additional polar smectic mesophase structures composed of layer stacks of different size (see Figure 8a–c).^[54]

Size effects of the silyl groups

Effects on the phase structure: Beside the layer decoupling, a second important effect of the Si-containing units is due to their size which becomes especially important for large Si-substituents at elevated temperature. In the compounds **Si1–Si3** and **CSi3** with bulky silyl units at both ends there is no possible way for the escape from this steric stress (Figure 5b). This leads to a frustration of the smectic layers with formation of columnar ribbon phases (Col_{ob}) at higher temperature (compounds **Si3**, **Si3i** and **CSi3**). The size of the ribbons is reduced with increasing steric frustration (compare the linear compound **Si3** and the branched compound **Si3i**). Because the molecules are tilted in the layers, the ribbons organize into an oblique lattice. In these oblique ribbon phases any anticlinic organization is highly unfavorable due to packing constraints at the inter-ribbon interfaces. Therefore, all anticlinic defects are squeezed out and the organization of the molecules in these columnar phases is exclusively synclinic.

As the temperature is reduced, this steric effect becomes smaller, the inter-ribbon interfaces disappear and infinite smectic layers are formed. In these smectic phases (SmCP_A , USmCP_A) anticlinic interfaces become possible which immediately gives rise to a $[\text{SmC}_s\text{P}_F]_a\text{P}_A$ structure of these smectic phases, indicated by a texture with extinction crosses parallel to the polarizers.

Effects on the switching process: The steric effects provided by the Si-containing end-groups should also be responsible for the change of the switching process, which can take place either by a collective rotation on a cone or around the long axis (Figure 2d,e). As a close packing is not possible for molecules with silyl groups at both ends more space becomes available between the bent cores and therefore not only in the columnar phases where the switching around the cone is inhibited by the inter-ribbon interfaces, but also in the smectic phases of compounds **Si2**, **Si3**, **Si3i** and **CSi3** the switching always takes place by rotation around the long axis (with exception of the switching of compound **Si1** with the smallest silyl group at $T < 110^\circ\text{C}$). This type of switching is of special interest as it changes the chirality sense of the layers and hence allows the switching of the superstructural chirality.

For compound **Si3** the steric effects are even large enough to give rise to a transition from an AF switching ($\text{Col}_{\text{ob}}\text{P}_A$) to a nonswitching columnar (Col_{ob}) phase upon rising the temperature. This means that there is a temperature dependent transition from a polar ordered to a conventional non-polar phase. Though this was previously reported for smectic phases,^[55] this phenomenon is rare in columnar phases.

There is only one report about such a transition in a hexagonal columnar phase of a polycatenar bent-core molecule, but the proposed phase structure of these Col_h phases is different from that one of the Col_{ob} phases reported herein.^[56]

Especially in the smectic phase occurring directly below the $\text{Col}_{ob}P_A$ phase there is still a significant steric frustration which separates the bent-cores of the individual molecules in the smectic layers. In these smectic phases the layer polarization is comparatively small. Dielectric measurements (Figure 16) indicate that the rotation around the long axis is quite easy and hence the polarization within the SmC_sP_F

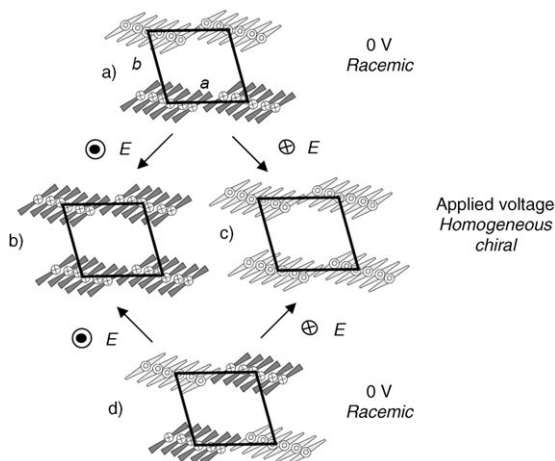


Figure 18. Modes of organization in the $\text{Col}_{ob}P_A$ phases, the number of molecules in the ribbons and the tilt direction of the molecules with respect to b were arbitrarily chosen (the molecules could also be organized more parallel to b). a) AF organization with alternation of the polar direction between the modulated layers. b) FE organization. c) FE organization with opposite polarity and chirality. d) AF organization with alternation of the polar direction from ribbon to ribbon within the modulated layers.

layer stacks of the $[\text{SmC}_sP_F]_aP_A$ structure is not large enough to allow a sufficiently strong coupling of these layer stacks to the surfaces and the switching process is AF. Only upon further reduction of the temperature the polarization increases and at a certain temperature the polar surface interactions become strong enough to induce FE switching.

Effects of the phase structure on the switching behavior

An additional important effect of the organization of the molecules in a ribbon structure is the change of the switching process from surface stabilized FE in the smectic phases (SmCP_{FE}) to AF in the columnar phases ($\text{Col}_{ob}P_A$). In order to understand this it must be considered that there are two principally different organizations which can lead to antiferroelectricity in the ribbon phases. Either the polar direction changes along the direction b between the modulated layers as shown in Figure 18a, or the antipolar order is realized within the modulated layers from ribbon to ribbon (i.e., along the direction a), as shown in Figure 18d. As seen in Figure 18 the ribbon structure can be achieved if there is an

overlapping of about one half of the rigid bent cores at the interfaces between adjacent ribbons. In this way the inter-ribbon interfaces of the AF arrangements Figure 18a and d become different. Only the reversal of the polar directions within the modulated layers (along direction a , as in Figure 18d) allows a parallel packing of the rod-like wings of the aromatic cores at the interfaces between the ribbons. This enables a continuous packing of the rod-like wings in adjacent ribbons and therefore this organization seems to be favorable. In contrast, if the polar direction in adjacent ribbons would be synpolar (FE, see Figure 18b,c), then the rod-like wings are not parallel at these interfaces and therefore unfavorable packing results at these interfaces. Hence, it can be concluded that in the $\text{Col}_{ob}P_A$ phases the polar direction changes within the modulated layers from ribbon to ribbon, as shown in Figure 18d. This also means that a FE organization, which requires a uniform polar order along direction a (Figure 18b,c) is less favorable than the AF structure (Figure 18d). Therefore, the switching process changes from FE in smectic phases (continuous layers) to AF in the Col_{ob} type ribbon phases. For the same reason the switching of the AF ground state into the FE state requires significant energy and the threshold voltage for this switching process becomes much higher than in the smectic phases.

It can be concluded, that the fundamental mode of switching of the silylated bent-core molecules with a sufficiently large number of dimethylsilyl groups is surface stabilized FE (SmCP_{FE} phases). AF switching is the result of the steric frustration arising from very large silyl groups, either leading to the formation of unfavorable inter-ribbon interfaces ($\text{Col}_{ob}P_A$ phases), or to the separation of the bent cores in the layers which reduces the polar order and hence decreases the surface coupling (SmCP_A and USmCP_A phases).

In summary, a significant step forward was achieved in the understanding of the self organization of bent-core molecules in general. The proposed models, based on a mesophase structure composed of chiral and polar mesoscale SmC_sP_F layer stacks with anticlinic defects, provide a quite uniform picture and allow the explanation of the different observations made within the distinct series of silylated bent-core compounds reported herein and earlier.^[16,19] It contributes to a fundamental understanding of the dark conglomerate phases and the transition from AF to FE switching. It also provides new insights into the general relations between structure and properties of chevron shaped molecules which allow a more efficient design of soft matter materials with ferroelectric/antiferroelectric properties and switchable supramolecular (superstructural) chirality for use in future applications.

Experimental Section

Methods: Determination of phase transition temperatures was done by polarizing microscopy (Optiphot-2 polarizing microscope, Nikon in conjunction with a FP 82 HT hot stage, Mettler) and confirmed by DSC (DSC-7, Perkin-Elmer, scanning rate 10 K min^{-1}). Powder X-ray investi-

gations were carried out with a Guinier film camera and a Guinier goniometer (both by Huber) with samples kept in glass capillaries ($\varnothing = 1$ mm) in a temperature-controlled heating stage using quartz-monochromatized $\text{Cu}_{\text{K}\alpha}$ radiation (30 to 60 min exposure time, calibration of the film patterns with the powder pattern of $\text{Pb}(\text{NO}_3)_2$). 2D patterns for aligned samples on a glass plate on a temperature-controlled heating stage (alignment at the sample/glass or at the sample/air interface) were recorded with a 2D detector (HI-STAR, Siemens). Electrooptical measurements were carried out in commercial ITO cells (E. H. C. Corp.; spacing: 5 μm or 6 μm). The switching polarization was measured by means of the triangular wave voltage method.^[57] Dielectric investigations were carried out in the range from 1 Hz to 10 MHz using a Solartron-Schlumberger Impedance Analyzer Si 1260 and a Chelsea Interface. A brass cell coated with gold ($d = 0.2$ mm) was used as capacitor.

Synthesis and analytical data

En: 3,4'-Biphenyldiol^[24] (0.5 g, 2.7 mmol), 4-[4-(undec-10-enyloxy)benzoyloxy]benzoic acid^[25] (2.32 g, 5.7 mmol), DCC (1.17 g, 5.7 mmol) and DMAP (0.05 g) were dissolved in dry CH_2Cl_2 (80 mL) and stirred at room temperature for 24 h. After evaporation of the solvent the crude product was purified by column chromatography (CHCl_3 , $R_f = 0.22$). Yield: 1.89 g (72%), colourless solid. $^1\text{H NMR}$ (400 MHz, CDCl_3): $\delta = 8.29$ (m, 4H, Ar-H), 8.14 (d, $^3J = 8.5$ Hz, 4H, Ar-H), 7.65 (d, $^3J = 8.7$ Hz, 2H, Ar-H), 7.51 (m, 2H, Ar-H), 7.47 (m, 1H, Ar-H), 7.37 (m, 4H, Ar-H), 7.31 (d, $^3J = 8.7$ Hz, 2H, Ar-H), 7.21 (m, 1H, Ar-H), 6.97 (d, $^3J = 8.9$ Hz, 4H, Ar-H), 5.81 (m, 2H, $\text{CH}=\text{CH}_2$), 4.95 (m, 4H, $\text{CH}=\text{CH}_2$), 4.04 (t, $^3J = 6.6$ Hz, 4H, OCH_2), 2.02 (m, 4H, $\text{CH}_2-\text{CH}=\text{CH}_2$), 1.81 (m, 4H, OCH_2CH_2), 1.33 (m, 20H, CH_2).

Si1: Under an argon atmosphere **En** (300 mg, 0.31 mmol) was dissolved in anhydrous toluene (5 mL), ethyldimethylsilane (120 mg, 1.3 mmol) and one drop of Karstedt's catalyst (platinum-divinyltetramethyl-siloxane complex in xylene, Gelest Inc.) was added to this mixture. After reaction was completed (detection by TLC, ca. 36 h) the solvent was evaporated and the crude product was purified by centrifugal preparative thin layer chromatography (silica gel, CHCl_3) followed by recrystallisation from ethyl acetate to give **Si1** (60 mg, 0.14 g, 32%). $^1\text{H NMR}$ (400 MHz, CDCl_3): $\delta = 8.29$ (d, $^3J = 8.7$ Hz, 2H, Ar-H), 8.15 (d, $^3J = 8.7$ Hz, 4H, Ar-H), 7.63 (d, $^3J = 8.5$ Hz, 2H, Ar-H), 7.49 (d, $^3J = 4.9$ Hz, 2H, Ar-H), 7.44 (m, 1H, Ar-H), 7.36 (d, $^3J = 8.7$ Hz, 2H, Ar-H), 7.27 (d, $^3J = 8.7$ Hz, 2H, Ar-H), 7.21 (m, 1H, Ar-H), 6.97 (d, 4H, $^3J = 8.9$ Hz, Ar-H), 4.04 (t, $^3J = 6.5$ Hz, 4H, OCH_2), 1.82 (m, 4H, OCH_2CH_2), 1.45 (m, 4H, $\text{OCH}_2\text{CH}_2\text{CH}_2$), 1.25 (m, 30H, CH_2), 0.44 (m, 4H, SiCH_2), 0.05 [s, 36H, $\text{Si}(\text{CH}_3)_3$], -0.02 (s, 6H, $\text{Si}-\text{CH}_3$); $^{13}\text{C NMR}$ (125 MHz, CDCl_3): $\delta = 164.32$ (4C), 164.18 (2C), 163.73 (2C), 155.36 (2C), 151.27, 150.59, 142.00, 137.96, 132.34 (4C), 131.75 (4C), 129.78, 128.25 (2C), 126.78 (2C), 124.62, 122.05 (4C), 122.01 (4C), 120.95, 120.55, 120.39, 114.40, 68.44 (2C), 33.29 (2C), 29.69 (2C), 29.65 (4C), 29.44 (4C), 29.19 (2C), 26.08 (2C), 23.16 (2C), 17.74 (2C), 1.97 (12C), -0.14 (2C); $^{29}\text{Si NMR}$ (99.3 MHz, CDCl_3): $\delta = 3.6$; elemental analysis calcd (%) for $\text{C}_{70}\text{H}_{90}\text{O}_{10}\text{Si}_2$: C 73.26, H 7.90; found: C 73.56, H 7.78.

Si2: $^1\text{H NMR}$ (400 MHz, CDCl_3): $\delta = 8.29$ (d, $^3J = 8.9$ Hz, 2H, Ar-H), 8.28 (d, $^3J = 8.9$ Hz, 2H, Ar-H), 8.14 (d, $^3J = 8.5$ Hz, 4H, Ar-H), 7.65 (d, $^3J = 8.7$ Hz, 2H, Ar-H), 7.51 (d, $^3J = 4.8$ Hz, 2H, Ar-H), 7.44 (m, 1H, Ar-H), 7.37 (d, $^3J = 8.7$ Hz, 2H, Ar-H), 7.36 (d, $^3J = 8.9$ Hz, 2H, Ar-H), 7.29 (d, $^3J = 8.7$ Hz, 2H, Ar-H), 7.22 (m, 1H, Ar-H), 6.97 (d, 4H, $^3J = 9.1$ Hz, Ar-H), 4.04 (m, 4H, OCH_2), 1.82 (m, 4H, OCH_2CH_2), 1.45 (m, 4H, $\text{OCH}_2\text{CH}_2\text{CH}_2$), 1.25 (m, 28H, CH_2), 0.49 (m, 4H, SiCH_2), 0.05 [s, 18H, $\text{Si}(\text{CH}_3)_3$], 0.02 [s, 12H, $\text{Si}(\text{CH}_3)_2$]; $^{13}\text{C NMR}$ (125 MHz, CDCl_3): $\delta = 164.47$ (4C), 164.45, 164.31, 163.83, 155.44 (2C), 151.34, 150.65, 142.07, 138.02, 132.41, 131.83 (8C), 129.86, 128.32 (2C), 126.85, 126.82, 124.69, 122.11 (4C), 122.07 (4C), 120.96, 120.62, 120.44, 114.42, 68.39 (2C), 33.40 (2C), 29.61 (2C), 29.56 (2C), 29.55 (2C), 29.37 (2C), 29.09 (2C), 25.98 (2C), 23.26 (2C), 23.17 (2C), 18.37, 18.13, 1.97 (6C), 0.35 (4C); $^{29}\text{Si NMR}$ (99.3 MHz, CDCl_3): $\delta = 6.16$, 5.34; elemental analysis calcd (%) for $\text{C}_{72}\text{H}_{98}\text{O}_{12}\text{Si}_4$: C 68.21, H 7.79; found: C 68.67, H 7.67.

Si3: $^1\text{H NMR}$ (400 MHz, CDCl_3): $\delta = 8.29$ (d, $^3J = 8.7$ Hz, 2H, Ar-H), 8.28 (d, $^3J = 8.7$ Hz, 2H, Ar-H), 8.14 (d, $^3J = 8.7$ Hz, 4H, Ar-H), 7.65 (d, $^3J = 8.5$ Hz, 2H, Ar-H), 7.49 (d, $^3J = 5.2$ Hz, 2H, Ar-H), 7.44 (m, 1H, Ar-H), 7.37 (d, $^3J = 8.7$ Hz, 2H, Ar-H), 7.36 (d, $^3J = 8.7$ Hz, 2H, Ar-H), 7.29

(d, $^3J = 8.7$ Hz, 2H, Ar-H), 7.21 (m, 1H, Ar-H), 6.97 (d, 4H, $^3J = 8.9$ Hz, Ar-H), 4.04 (t, $^3J = 6.6$ Hz, 4H, OCH_2), 1.81 (m, 4H, OCH_2CH_2), 1.47 (m, 4H, $\text{OCH}_2\text{CH}_2\text{CH}_2$), 1.27 (m, 28H, CH_2), 0.50 (m, 2H, SiCH_2), 0.07 [s, 18H, $\text{Si}(\text{CH}_3)_3$], 0.04 [s, 12H, $\text{Si}(\text{CH}_3)_2$], 0.02 [s, 12H, $\text{Si}(\text{CH}_3)_2$]; $^{13}\text{C NMR}$ (125 MHz, CDCl_3): $\delta = 164.49$ (4C), 164.47, 164.33, 163.84, 155.45 (2C), 151.35, 150.66, 142.09, 138.04, 132.42, 131.84 (8C), 129.87, 128.33 (2C), 126.82 (2C), 124.71, 122.12 (4C), 122.08 (4C), 120.97, 120.63, 120.45, 114.43, 68.40 (2C), 33.44 (2C), 29.62 (2C), 29.58 (2C), 29.56 (2C), 29.39 (2C), 29.37 (2C), 29.09 (2C), 25.99 (2C), 23.23 (2C), 18.29 (2C), 1.81 (6C), 1.27 (4C), 0.20 (4C); $^{29}\text{Si NMR}$ (99.3 MHz, CDCl_3): $\delta = 7.47$, 7.03, -21.06 ; elemental analysis calcd (%) for $\text{C}_{76}\text{H}_{110}\text{O}_{14}\text{Si}_6$: C 64.46, H 7.83; found: C 64.29, H 7.6.

CSi3: $^1\text{H NMR}$ (400 MHz, CDCl_3): $\delta = 8.29$ (d, $^3J = 8.9$ Hz, 2H, Ar-H), 8.28 (d, $^3J = 8.7$ Hz, 2H, Ar-H), 8.14 (d, $^3J = 8.7$ Hz, 4H, Ar-H), 7.65 (d, $^3J = 8.9$ Hz, 2H, Ar-H), 7.51 (d, $^3J = 5.2$ Hz, 2H, Ar-H), 7.44 (m, 1H, Ar-H), 7.37 (d, $^3J = 8.7$ Hz, 2H, Ar-H), 7.36 (d, $^3J = 8.7$ Hz, 2H, Ar-H), 7.28 (d, $^3J = 8.7$ Hz, 2H, Ar-H), 7.22 (m, 1H, Ar-H), 6.97 (d, 4H, $^3J = 8.9$ Hz, Ar-H), 4.04 (t, $^3J = 6.5$ Hz, 4H, OCH_2), 1.81 (m, 4H, OCH_2CH_2), 1.47 (m, 4H, $\text{OCH}_2\text{CH}_2\text{CH}_2$), 1.32 (m, 38H, CH_2), 0.53 (m, 16H, SiCH_2), 0.46 (m, 4H, SiCH_2), -0.04 [s, 18H, $\text{Si}(\text{CH}_3)_3$], -0.07 [s, 24H, $\text{Si}(\text{CH}_3)_2$]; $^{13}\text{C NMR}$ (125 MHz, CDCl_3): $\delta = 164.46$ (4C), 164.43 (2C), 164.29, 163.83, 155.43 (2C), 151.34, 150.65, 142.06, 138.01, 132.41, 131.82 (4C), 131.57 (4C), 129.85, 128.31 (2C), 126.85, 126.81, 124.68, 124.61, 122.11 (2C), 122.07 (2C), 120.96, 120.62, 120.44, 114.42, 68.39 (2C), 33.70 (2C), 29.63 (2C), 29.59 (2C), 29.55 (2C), 29.37 (2C), 29.29 (2C), 29.09 (2C), 25.98 (2C), 23.92 (2C), 21.36 (2C), 20.10 (2C), 20.03 (2C), 20.00 (2C), 18.41 (4C), 15.38 (2C), -1.54 (6C), -3.18 (4C), -3.26 (4C); $^{29}\text{Si NMR}$ (99.3 MHz, CDCl_3): $\delta = 1.59$, 0.99, 0.57; elemental analysis calcd (%) for $\text{C}_{88}\text{H}_{134}\text{O}_{10}\text{Si}_6$: C 69.5, H 8.88; found: C 70.05, H 8.86.

Acknowledgements

The work was supported by the DFG (GRK 894/1) and the Fonds der Chemischen Industrie; R.A.R. is grateful to the Alexander von Humboldt Foundation for the research fellowship.

- [1] a) J.-M. Lehn, *Proc. Natl. Acad. Sci. USA* **2002**, *99*, 4763–4768; b) J.-M. Lehn, *Science* **2002**, *295*, 2400–2403.
- [2] V. A. Blatov, L. Carlucci, G. Ciani, D. M. Proserpio, *CrystEngComm* **2004**, *6*, 377–395.
- [3] B. Moulton, M. J. Zaworotko, *Chem. Rev.* **2001**, *101*, 1629–1658.
- [4] a) D. M. Bassani, J.-M. Lehn, K. Fromm, D. Fenske, *Angew. Chem.* **1998**, *110*, 2534–2537; *Angew. Chem. Int. Ed.* **1998**, *37*, 2364–2567; b) P. N. W. Baxter, J.-M. Lehn, G. Baum, D. Fenske, *Chem. Eur. J.* **2000**, *6*, 4510–4517; c) E. Breuning, G. S. Hanan, F. J. Romero-Salguero, A. M. Garcia, P. N. W. Baxter, J.-M. Lehn, E. Wegelius, K. Rissanen, H. Nierengarten, A. van Dorsselaer, *Chem. Eur. J.* **2002**, *8*, 3458–3466.
- [5] S. R. Seidel, P. J. Stang, *Acc. Chem. Res.* **2002**, *35*, 972–983.
- [6] *Handbook of Liquid Crystals, Vol. 1–3* (Eds.: D. Demus, J. Goodby, G. W. Gray, H.-W. Spiess, V. Vill), Wiley-VCH, Weinheim, **1998**.
- [7] a) T. Yamamoto, A. M. Arif, P. Stang, *J. Am. Chem. Soc.* **2003**, *125*, 12309–12317; b) M. Fujita, *Chem. Soc. Rev.* **1998**, *27*, 417–425.
- [8] a) M. T. Stone, J. M. Heemstra, J. S. Moore, *Acc. Chem. Res.* **2006**, *39*, 11–20; b) H.-J. Kim, W.-C. Zin, M. Lee, *J. Am. Chem. Soc.* **2004**, *126*, 7009–7014.
- [9] B. Hasenknopf, J.-M. Lehn, *Helv. Chim. Acta* **1996**, *79*, 1643–1650.
- [10] H. Abourahma, B. Moulton, V. Kravtsov, M. J. Zaworotko, *J. Am. Chem. Soc.* **2002**, *124*, 9990–9991.
- [11] M. Tominaga, K. Suzuki, T. Murase, M. Fujita, *J. Am. Chem. Soc.* **2005**, *127*, 11950–11951.
- [12] T. Niori, T. Sekine, J. Watanabe, T. Furukawa, H. Takezoe, *J. Mater. Chem.* **1996**, *6*, 1231–1233.
- [13] Reviews: a) G. Pelzl, S. Diele, W. Weissflog, *Adv. Mater.* **1999**, *11*, 707–724; b) C. Tschierske, G. Dantlgraber, *Pramana* **2003**, *61*, 455–481; c) R. Amaranatha Reddy, C. Tschierske, *J. Mater. Chem.* **2006**,

- 16, 907–961; d) M. B. Ros, J. L. Serrano, M. R. de la Fuente, C. L. Folcia, *J. Mater. Chem.* **2005**, *15*, 5093–5098; e) H. Takezoe, Y. Takahashi, *Jpn. J. Appl. Phys.* **2006**, *45*, 597–625.
- [14] a) D. R. Link, G. Natale, R. Shao, J. E. MacLennan, N. A. Clark, E. Körblová, D. M. Walba, *Science* **1997**, *278*, 1924–1927; b) D. M. Walba, *Top. Stereochem.* **2003**, *42*, 475–518.
- [15] Examples of FE switching bent-core materials: a) D. M. Walba, E. Körblová, R. Shao, J. E. MacLennan, D. R. Link, M. A. Glaser, N. A. Clark, *Science* **2000**, *288*, 2181–2184; b) E. Gorecka, D. Pociecha, F. Araoka, D. R. Link, M. Nakata, J. Thisayukta, Y. Takahashi, K. Ishikawa, J. Watanabe, H. Takezoe, *Phys. Rev. E* **2000**, *62*, R4524–R4527; c) M. Nakata, D. R. Link, F. Araoka, J. Thisayukta, Y. Takahashi, K. Ishikawa, J. Watanabe, H. Takezoe, *Liq. Cryst.* **2001**, *28*, 1301–1308; d) J. P. Bedel, J. C. Rouillon, J. P. Marcerou, M. Laguerre, H. T. Nguyen, M. F. Achard, *J. Mater. Chem.* **2002**, *12*, 2214–2220; e) R. Amaranatha Reddy, B. K. Sadashiva, *J. Mater. Chem.* **2002**, *12*, 2627–2642; f) R. Amaranatha Reddy, B. K. Sadashiva, *Liq. Cryst.* **2003**, *30*, 1031–1050; g) S. Rauch, P. Bault, H. Sawade, G. Heppke, G. G. Nair, A. Jakli, *Phys. Rev. E* **2002**, *66*, 021706; h) K. Kumazawa, M. Nakata, F. Araoka, Y. Takahashi, K. Ishikawa, J. Watanabe, H. Takezoe, *J. Mater. Chem.* **2004**, *14*, 157–164; i) R. Amaranatha Reddy, V. A. Raghunathan, B. K. Sadashiva, *Chem. Mater.* **2005**, *17*, 274–283; j) H. Nadasi, W. Weissflog, A. Eremin, G. Pelzl, S. Diele, S. Das, S. Grande, *J. Mater. Chem.* **2002**, *12*, 1316–1324; k) J. P. Bedel, J. C. Rouillon, J. P. Marcerou, H. T. Nguyen, M. F. Achard, *Phys. Rev. E* **2004**, *69*, 061702; l) T. S. K. Lee, S. Heo, J. G. Lee, K.-T. Kang, K. Kumazawa, K. Nishida, Y. Shimbo, Y. Takahashi, J. Watanabe, T. Doi, T. Takahashi, H. Takezoe, *J. Am. Chem. Soc.* **2005**, *127*, 11085–11091.
- [16] Preliminary communication (compound **Si3f**):^[28] C. Keith, R. Amaranatha Reddy, U. Baumeister, C. Tschierske, *J. Am. Chem. Soc.* **2004**, *126*, 14312–14313.
- [17] a) M. W. Schröder, S. Diele, G. Pelzl, W. Weissflog, *ChemPhysChem* **2004**, *5*, 99–103; b) R. Amaranatha Reddy, M. W. Schröder, M. Bodyagin, H. Kresse, S. Diele, G. Pelzl, W. Weissflog, *Angew. Chem.* **2005**, *117*, 784–788; *Angew. Chem. Int. Ed.* **2005**, *44*, 774–778; c) J. P. Bedel, J. C. Rouillon, J. P. Marcerou, H. T. Nguyen, M. F. Achard, *Phys. Rev. E* **2004**, *69*, 061702; d) E. Gorecka, N. Vaupotic, D. Pociecha, M. Cepic, J. Mieczkowski, *ChemPhysChem* **2005**, *6*, 1087–1093.
- [18] a) A. Jakli, *Liq. Cryst. Today* **2002**, *11*, 1–5; b) A. Jakli, L.-C. Chien, D. Krüerke, H. Sawade, G. Heppke, *Liq. Cryst.* **2002**, *29*, 377–381; c) F. Kentischer, R. Macdonald, P. Warnick, G. Heppke, *Liq. Cryst.* **1998**, *25*, 341–347.
- [19] a) G. Dantlgraber, A. Eremin, S. Diele, A. Hauser, H. Kresse, G. Pelzl, C. Tschierske, *Angew. Chem.* **2002**, *114*, 2515–2518; *Angew. Chem. Int. Ed.* **2002**, *41*, 2408–2412; b) G. Dantlgraber, S. Diele, C. Tschierske, *Chem. Commun.* **2002**, 2768–2769; c) G. Dantlgraber, U. Baumeister, S. Diele, H. Kresse, B. Lühmann, H. Lang, C. Tschierske, *J. Am. Chem. Soc.* **2002**, *124*, 14852–14853; d) C. Keith, R. Amaranatha Reddy, H. Hahn, H. Lang, C. Tschierske, *Chem. Commun.* **2004**, 1898–1899; e) C. Keith, R. Amaranatha Reddy, C. Tschierske, *Chem. Commun.* **2005**, 871–873; f) C. Keith, R. Amaranatha Reddy, A. Hauser, U. Baumeister, C. Tschierske, *J. Am. Chem. Soc.* **2006**, *128*, 3051–3066; g) R. Amaranatha Reddy, G. Dantlgraber, U. Baumeister, C. Tschierske, *Angew. Chem.* **2006**, *118*, 1962–1967; *Angew. Chem. Int. Ed.* **2006**, *45*, 1928–1933; h) C. Keith, R. Amaranatha Reddy, U. Baumeister, H. Hahn, H. Lang, C. Tschierske, *J. Mater. Chem.* **2006**, *16*, 3444–3447; i) H. Hahn, H. Lang, C. Keith, R. Amaranatha Reddy, C. Tschierske, *Adv. Mater.* **2006**, *18*, 2629–2633.
- [20] E. L. Eliel, S. H. Wilen, L. N. Mander, *Stereochemistry of Organic Compounds*, Wiley, New York, **1994**, p. 159.
- [21] There is a second different type of mesophases showing this type of “dark conglomerate textures”. In contrast to the mesophases discussed herein, which are simple layer structures without in-plane order, this second type has additional order and is assumed to be a soft crystalline phase, assigned as B4^[*], see D. M. Walba, L. Eshdat, E. Körblová, R. K. Shoemaker, *Cryst. Growth Des.* **2005**, *5*, 2091–2099, and references given in [30].
- [22] a) J. Thisayukta, Y. Nakayama, S. Kawachi, H. Takezoe, J. Watanabe, *J. Am. Chem. Soc.* **2000**, *122*, 7441–7448; b) J. Thisayukta, H. Kamee, S. Kawachi, J. Watanabe, *Mol. Cryst. Liq. Cryst.* **2000**, *346*, 63–75; c) H. N. Shreenivasa Murthy, B. K. Sadashiva, *Liq. Cryst.* **2002**, *29*, 1223–1234; d) J. Ortega, C. L. Folcia, J. Ettxebarria, N. Gimeno, M. B. Ros, *Phys. Rev. E* **2003**, *68*, 011707; e) W. Weissflog, M. W. Schröder, S. Diele, G. Pelzl, *Adv. Mater.* **2003**, *15*, 630–633; f) M. W. Schröder, S. Diele, G. Pelzl, U. Dunemann, H. Kresse, W. Weissflog, *J. Mater. Chem.* **2003**, *13*, 1877–1882; g) M. W. Schröder, G. Pelzl, U. Dunemann, W. Weissflog, *Liq. Cryst.* **2004**, *31*, 633–637; h) W. Weissflog, S. Sokolowski, H. Dehne, B. Das, S. Grande, M. W. Schröder, A. Eremin, S. Diele, G. Pelzl, H. Kresse, *Liq. Cryst.* **2004**, *31*, 923–933; i) V. Kozmik, A. Kovarova, M. Kuchar, J. Svoboda, V. Novotna, M. Glogarova, J. Kroupa, *Liq. Cryst.* **2006**, *33*, 41–56.
- [23] Field induced SmCP^[*] phases: a) G. Heppke, D. D. Parghi, H. Sawade, *Liq. Cryst.* **2000**, *27*, 313–320; b) J. Ettxebarria, C. L. Folcia, J. Ortega, M. B. Ros, *Phys. Rev. E* **2003**, *67*, 042702; c) A. Jakli, Y.-M. Huang, K. Fodor-Csorba, A. Vajda, G. Galli, S. Diele, G. Pelzl, *Adv. Mater.* **2003**, *15*, 1606–1610.
- [24] D. Shen, A. Pegenau, S. Diele, I. Wirth, C. Tschierske, *J. Am. Chem. Soc.* **2000**, *122*, 1593–1601.
- [25] R. Achten, A. Koudijs, M. Giesbers, A. T. M. Marcelis, E. J. R. Sudhölter, *Liq. Cryst.* **2005**, *32*, 277–285.
- [26] C. Tschierske, H. Zschke, *J. Prakt. Chem.* **1989**, *331*, 365–366.
- [27] However, the molecular length ($l=5.6$ nm, determined as described in footnote [c] in Table 1) is significantly larger than the parameter b and this is quite unusual in this case. A possible explanation could be that the molecules are not strictly orthogonal arranged within the ribbons, but adopt a tilted organization where the tilt direction changes randomly along the direction c . It is also possible that there is some intercalation of the terminally unsaturated chains which leads to a reduction of the efficient molecular length.
- [28] Re-indexation with improved X-ray data gave an oblique lattice with smaller lattice parameters than reported in a previous communication (ref. [16]).
- [29] The fact that only one diffuse scattering is found for the carbosilane **Si1** does not necessarily mean that in this case the Si-containing units are not segregated. The ethyldimethylsilyl groups (and also the carbosilane units in **CSi3**) provide the same mean distance as the alkyl chains. For this reason in the case of the investigated carbosilanes, the presence of a segregated structure cannot be deduced from the profile of the wide angle scattering.^[19h]
- [30] In thicker samples of compounds **Si1** and **Si2** a typical bluish color is seen. This type of “bluish conglomerate phases” was first reported for some bent-core molecules incorporating naphthalene units^[22a] and it was also seen for the soft crystalline B4^[*] phases: T. Sekine, T. Niori, J. Watanabe, T. Furukawa, S. W. Choi, H. Takezoe, *J. Mater. Chem.* **1997**, *7*, 1307–1309; H. Niwano, M. Nakata, J. Thisayukta, D. R. Link, H. Takezoe, J. Watanabe, *J. Phys. Chem. B* **2004**, *108*, 14889–14896; Thisayukta, H. Takezoe, J. Watanabe, *Jpn. J. Appl. Phys.* **2001**, *40*, 3277–3287; F. Araoka, N. Y. Ha, Y. Kinoshita, B. Park, J. W. Wu, H. Takezoe, *Phys. Rev. Lett.* **2005**, *94*, 137801. It might arise from a light scattering at disordered smectic domains.
- [31] K. D’Have, A. Dahlgren, P. Rudquist, J. P. F. Lagerwall, G. Andersson, M. Matuszczyk, S. T. Lagerwall, R. Dabrowski, W. Drzewinski, *Ferroelectrics* **2000**, *244*, 415–428.
- [32] For bent-core molecules a deviation from exactly 45° tilt angle (θ) is possible if the bending angle (α) is changed according to: $\alpha = 2 \tan^{-1}(1/\cos\theta)$.
- [33] G. Liao, S. Stojadinovic, G. Pelzl, W. Weissflog, S. Sprunt, A. Jakli, *Phys. Rev. E* **2005**, *72*, 021710.
- [34] M. Spannuth, L. Hough, D. Coleman, C. Jones, M. Nakata, Y. Takahashi, H. Takezoe, J. Watanabe, C. Tschierske, E. Körblová, D. Walba, N. A. Clark, Poster Presented at the *9th International Liquid Crystal Conference*, Ljubljana, July 4–9, **2004**, Book of Abstracts, SYN-P026.

- [35] Remarkably, also the birefringent textures obtained after shearing have a significantly lower viscosity than the original dark conglomerate phases of compounds **Si1** and **Si2**.
- [36] L. E. Hough, N. A. Clark, *Phys. Rev. Lett.* **2005**, *95*, 107802.
- [37] In a previous paper (see ref. [19f]) we have supported this proposal by the observation of a tilt-angle dependent inversion of the optical rotation, which is proposed by this model.
- [38] M. F. Achard, J. Ph. Bedel, J. P. Marcerou, H. T. Nguyen, J. C. Rouillon, *Eur. Phys. J. E* **2003**, *10*, 129–134.
- [39] In polyimide-coated cells the switching behavior can be more complex in some cases, due to the effect of an induced electric double layer, which will be discussed in section on the influence of surfaces.
- [40] In this notation the structure of the layer stacks is given in brackets and the following subscripts define the correlation between the layer stacks (a = antclinic, s = synclinic, A = antipolar, S = synpolar).
- [41] This kind of field induced texture was observed earlier in an AF switching smectic phase (SmCP_A): M. Zennoji, Y. Takanishi, K. Ishikawa, J. Thisayukta, J. Watanabe, H. Takezoe, *J. Mater. Chem.* **1999**, *9*, 2775–2778.
- [42] The symbol Ξ , according to the rules used by Beilstein, replaces stereochemical descriptors, in cases of configurational uncertainty and inhomogeneity, see *Stereochemical descriptors in Beilstein Handbook of Organic Chemistry*, Vol 18, Part 1, 4th ed., 5th Suppl., Springer, Berlin, **1986**, p. LXXV.
- [43] a) C. L. Folcia, J. Ortega, J. Etxebarria, *Liq. Cryst.* **2003**, *30*, 1189–1191; b) P. Pyc, J. Mieczkowski, D. Pocięcha, E. Gorecka, B. Donnio, D. Guillon, *J. Mater. Chem.* **2004**, *14*, 2374–2379.
- [44] The relaxation time decreases with increasing frequency of the applied AC field. The relaxation is very slow (i.e., it takes some minutes for completion) if the sample is aligned in a low frequency triangular wave field (10 Hz) and it becomes faster (several seconds) if the frequency is higher (100–500 Hz).
- [45] Such a zero voltage centered single peak switching was initially assigned to a superparaelectric switching process where macroscopic FE domains orient under the influence of the field, but are random without applied field: see reference [38]. The slow relaxation of the polar states to the dark texture can be regarded as such a type of reorganization. The dependence of the position of the peaks on the type of ITO-cell would mean that the fast switching process changes from FE in noncoated cells to superparaelectric in polyimide-coated cells. This is however in contradiction with the optical investigations, which indicate that in the polyimide coated cells, where a centered peak is observed, the birefringent texture is retained, whereas the (slow) relaxation to the random organization of the FE domains takes place in the noncoated ITO cells where a noncentered peak is observed. This makes an explanation of the peak position based on the effect of the internal (effective) field more reasonable.
- [46] S. Rauch, C. Selbmann, P. Bault, H. Sawade, G. Heppke, O. Morales-Saavedra, M. Y. M. Huang, A. Jakli, *Phys. Rev. E* **2004**, *69*, 021 707.
- [47] No supercooling of the phase transition Col_{ob}–SmCP_A was observed in X-ray experiments. Probably, the stronger surface interactions in the thin measurement cells (5–10 μm) used for the optical and electrooptical investigation provide a strong influence of these surfaces, which seems to stabilize the columnar organization. In X-ray diffraction experiments capillaries (Guinier method) or open droplets (2D X-ray) were used where the influence of the surfaces is diminished.
- [48] H. Kresse, H. Schlacken, U. Dunemann, M. W. Schröder, G. Pelzl, *Liq. Cryst.* **2002**, *29*, 1509–1512.
- [49] In polyimide coated ITO cells with the same thickness the transition was found at 126 °C, indicating for this compound a significant influence of the surfaces on this phase transition.
- [50] a) B. Zenks, M. Cipeć, *SPIE Proceedings* **1998**, *3318*, 68; b) T. Matsumoto, A. Fukuda, M. Johno, Y. Motoyama, T. Yui, S.-S. Seomun, M. Yamashita, *J. Mater. Chem.* **1999**, *9*, 2051–2080; c) M. A. Osipov, A. Fukuda, *Phys. Rev. E* **2000**, *62*, 3724–3735.
- [51] Based on the investigations reported herein it is suggested that also the monosilylated compounds **II** adopt a [SmC₃P_F]₃P_A ground-state structure in the dark conglomerate phases, instead of the initially proposed uniform SmC₃P_F structure.^[19f]
- [52] D. A. Coleman, J. Fernsler, N. Chattham, M. Nakata, Y. Takanishi, E. Korblova, D. R. Link, R.-F. Shao, W. G. Jang, J. E. MacLennan, O. Mondainn-Monval, C. Boyer, W. Weissflog, G. Pelzl, L.-C. Chien, J. Zasadzinski, J. Watanabe, D. M. Walba, H. Takezoe, N. A. Clark, *Science* **2003**, *301*, 1204–1211.
- [53] F. Araoka, H. Hoshi, H. Takezoe, *Phys. Rev. E* **2004**, *69*, 051 704.
- [54] A related sequence of structures resulting from SmC_aP_A layer stacks might also be possible for other materials.
- [55] a) I. Kovalenko, W. Weissflog, S. Grande, S. Diele, G. Pelzl, I. Wirth, *Liq. Cryst.* **2000**, *27*, 683–687; M. W. Schröder, S. Diele, N. Pancenko, W. Weissflog, G. Pelzl, *J. Mater. Chem.* **2002**, *12*, 1331–1334; b) J. Mieczkowski, K. Gomola, J. Koseska, D. Pocięcha, J. Szydłowska, E. Gorecka, *J. Mater. Chem.* **2003**, *13*, 2132–2137; c) A. Eremin, H. Nadasi, G. Pelzl, S. Diele, H. Kresse, W. Weissflog, S. Grande, *Phys. Chem. Chem. Phys.* **2004**, *6*, 1290–1298; d) H. N. Shreenivasa Murthy, B. K. Sadashiva, *Liq. Cryst.* **2004**, *31*, 567–578; e) W. Weissflog, U. Dunemann, M. W. Schröder, S. Diele, G. Pelzl, H. Kresse, S. Grande, *J. Mater. Chem.* **2005**, *15*, 939–946; f) R. Amaranatha Reddy, B. K. Sadashiva, U. Baumeister, *J. Mater. Chem.* **2005**, *15*, 3303–3316; g) J. P. F. Lagerwall, F. Giesselmann, M. D. Wand, D. M. Walba, *J. Mater. Chem.* **2004**, *14*, 3606–3615.
- [56] E. Gorecka, D. Pocięcha, J. Mieczkowski, J. Matraszek, D. Guillon, B. Donnio, *J. Am. Chem. Soc.* **2004**, *126*, 15946–15947.
- [57] K. Miyasato, S. Abe, H. Takezoe, A. Fukuda, E. Kuze, *Jpn. J. Appl. Phys.* **1983**, *22*, L661–L663.

Received: June 21, 2006
Published online: December 22, 2006